

Consequences of T-parity breaking in the Littlest Higgs model

A. FREITAS¹, P. SCHWALLER², D. WYLER²

¹ *Department of Physics & Astronomy, University of Pittsburgh,
3941 O'Hara St, Pittsburgh, PA 15260, USA*

² *Institut für Theoretische Physik, Universität Zürich,
Winterthurerstrasse 190, CH-8057 Zürich, Switzerland*

Abstract

In this paper we consider the effects of the T-parity violating anomalous Wess-Zumino-Witten-Term in the Littlest Higgs model. Apart from tree level processes, the loop induced decays of the heavy mirror particles into light standard model fermions lead to a new and rich phenomenology in particular at breaking scales f below 1 TeV. Various processes are calculated and their signatures at present and future colliders are discussed. As a byproduct we find an alternative production mechanism for the Higgs boson.

1 Introduction

Little Higgs models provide a mechanism to explain a hierarchy between the electroweak scale and a larger, fundamental scale where symmetry breaking occurs through strong dynamics. In this scheme, the Higgs scalar doublet is a composite particle of the strong dynamics, a pseudo-Goldstone boson stemming from the spontaneously broken symmetry at a scale f . The Goldstone mechanism protects the Higgs boson from acquiring a large mass term, with one-loop quadratic corrections being cancelled by new gauge bosons and partners of the top quark. A simple implementation of the Little Higgs concept with a single global symmetry group is the *Littlest* Higgs model [1]. However, owing to tree-level contributions of the new particles to the oblique electroweak parameters, electroweak precision data requires f to be above 5 TeV [2]. On the other hand a scale as low as 1 TeV is required to avoid fine-tuning of the Higgs mass.

This problem can be circumvented by imposing a discrete symmetry, called *T-parity* [3,4]. Under this symmetry, the Standard Model (SM) fields are T-even, while the new TeV-scale particles are odd, effectively forbidding all tree-level interactions between one of the new heavy degrees of freedom and SM particles. Therefore, the new particles can only be generated in pairs, which is reminiscent of R-parity in supersymmetric theories. Besides satisfying the electroweak constraints even for $f < 1$ TeV, an exactly realized T-parity also leads to the lightest T-odd particle being stable and, if neutral, a good candidate for (cold) dark matter.

However, it was pointed out by Hill and Hill [5,6] that typical models of strongly interacting symmetry breaking would lead to a Wess-Zumino-Witten (WZW) term [7] which is odd under T-parity¹. The structure of the WZW term can be derived from topological considerations and depends only on the pattern of the global and gauged symmetry groups. The breaking of T-parity by the WZW term, though suppressed by the large symmetry breaking scale, rules out the lightest T-odd particle as a dark matter candidate, since this particle would decay promptly into gauge bosons [10]. Nevertheless, if the WZW term is a priori the only source of T-parity breaking, the electroweak precision constraints could still be satisfied.

In this paper, we analyze the effect of the WZW term in the Littlest Higgs model with T-parity (LHT) further. The relevant interactions induced by this term are derived, and their gauge invariance is shown. Furthermore, it is demonstrated that the WZW term cannot be the only T-parity violating operator, but that other T-odd terms are needed in the Lagrangian to make the theory consistent. Equipped with these results, we discuss the constraints on the model from LEP and Tevatron data and comment on the surprisingly rich phenomenological prospects for LHC.

After reviewing the LHT model and specifying the notations in section 2, the T-odd interactions induced by the WZW term are studied in section 3. In section 4 the T-parity violating signals at LEP and hadron colliders are investigated. Finally, conclusions are given in section 5.

¹It is possible to construct models which do not have WZW terms or where T-parity is not broken by these terms [8,9]. This avenue will not be explored further in this paper.

2 The Littlest Higgs model with T-parity

Here the main aspects of the model are reviewed, following the detailed description in Refs. [11, 12].

The Littlest Higgs model is based on a $SU(5)/SO(5)$ symmetry breaking pattern. A global $SU(5)$ symmetry is broken down to $SO(5)$ by a vacuum expectation value of the form

$$\langle \Sigma \rangle = \Sigma_0 = \begin{pmatrix} & & 1 & & \\ & & & 1 & \\ & 1 & & & \\ 1 & & & & \\ & & 1 & & \end{pmatrix} \quad (1)$$

for a field Σ transforming in the two-index symmetric representation of $SU(5)$. The generators of $SU(5)$ are split up into a set of ten unbroken generators T^a that generate the unbroken $SO(5)$ subgroup and a set of 14 broken generators X^a .

The Goldstone modes of the broken generators are implemented in a non-linear sigma model with a breaking scale f ,

$$\mathcal{L}_\Sigma = \frac{f^2}{4} \text{Tr} |D_\mu \Sigma|^2, \quad (2)$$

with

$$\Sigma = e^{i\Pi/f} \Sigma_0 e^{i\Pi^\top/f} = e^{2i\Pi/f} \Sigma_0, \quad (3)$$

where $\Pi = \pi_a X^a$ is the Goldstone matrix. A $[SU(2) \times U(1)]^2$ subgroup of $SU(5)$ is gauged [1], with associated gauge bosons $W_{1,2}^a$ and $B_{1,2}$, respectively. In terms of 2×2 , 1×1 and 2×2 blocks, the gauge group generators are given by

$$Q_1^a = \begin{pmatrix} \sigma^a/2 & 0 & 0 \\ 0 & 0 & 0 \\ 0 & 0 & 0 \end{pmatrix}, \quad Y_1 = \frac{1}{10} \begin{pmatrix} 3 & 0 & 0 \\ 0 & -2 & 0 \\ 0 & 0 & -2 \end{pmatrix}, \quad (4)$$

$$Q_2^a = \begin{pmatrix} 0 & 0 & 0 \\ 0 & 0 & 0 \\ 0 & 0 & -\sigma^{a*}/2 \end{pmatrix}, \quad Y_2 = \frac{1}{10} \begin{pmatrix} 2 & 0 & 0 \\ 0 & 2 & 0 \\ 0 & 0 & -3 \end{pmatrix}, \quad (5)$$

where σ^a , $a = 1, 2, 3$ are the Pauli matrices. The covariant derivative reads

$$D_\mu \Sigma \equiv \partial_\mu \Sigma - \sum_{k=1,2} [g_k W_{k,\mu}^a (Q_k^a \Sigma + \Sigma Q_k^{aT}) + g'_k B_{k,\mu} (Y_k \Sigma + \Sigma Y_k)]. \quad (6)$$

The vacuum Σ_0 breaks the gauge symmetry $[SU(2) \times U(1)]^2$ down to the diagonal subgroup, giving one set of gauge bosons with masses of order f , while the other set remains massless at this stage and is identified with the Standard Model gauge bosons. The Goldstone matrix Π is explicitly given by

$$\Pi = \begin{pmatrix} \omega/2 - \eta/\sqrt{20} \mathbb{1} & H/\sqrt{2} & \Phi \\ H^\dagger/\sqrt{2} & \sqrt{4/5} \eta & H^\top/\sqrt{2} \\ \Phi^\dagger & H^*/\sqrt{2} & \omega^\dagger/2 - \eta/\sqrt{20} \mathbb{1} \end{pmatrix}, \quad (7)$$

where H is the Little Higgs doublet, Φ is a complex triplet under $(\text{SU}(2) \times \text{U}(1))_{SM}$, which receives a mass of $\mathcal{O}(f)$, and the real triplet field $\omega = \omega^a \sigma^a$ and the real singlet η are eaten by the heavy gauge bosons ($\mathbb{1}$ is the 2×2 identity matrix).

The Littlest Higgs model can be supplemented by a discrete Z_2 symmetry called T-parity [4], with SM particles being even ($T = +1$), and non-SM particles odd ($T = -1$) under this symmetry. Their couplings to the non-linear sigma fields generate masses of order f for the T-odd particles. In the gauge sector, T-parity is realized by the automorphism $T^a \rightarrow T^a$ and $X^a \rightarrow -X^a$. As a result, T-parity interchanges the two sets of gauge bosons,

$$W_1^a \leftrightarrow W_2^a, \quad B_1 \leftrightarrow B_2. \quad (8)$$

T-parity requires the two sets of gauge couplings to be identical: $g_1 = g_2 = \sqrt{2}g$ and $g'_1 = g'_2 = \sqrt{2}g'$. The gauge bosons form a light and a heavy linear combination:

$$W_L^a = \frac{1}{\sqrt{2}}(W_1^a + W_2^a), \quad (\text{T-even}) \quad (9)$$

$$B_L = \frac{1}{\sqrt{2}}(B_1 + B_2), \quad (10)$$

with masses from usual electroweak symmetry breaking, and

$$W_H^a = \frac{1}{\sqrt{2}}(W_1^a - W_2^a), \quad (\text{T-odd}) \quad (11)$$

$$B_H = \frac{1}{\sqrt{2}}(B_1 - B_2), \quad (12)$$

with masses of order f generated from the kinetic term of the non-linear sigma model. After electroweak symmetry breaking, the light gauge bosons mix to form the usual physical states of the SM, $A_L = c_W B_L - s_W W_L^3$, $Z_L = s_W B_L + c_W W_L^3$ and $W_L^\pm = (W_L^1 \mp W_L^2)/\sqrt{2}$. Here, as usual, s_W and c_W denote the sine and cosine of the weak mixing angle. Similarly, a small mixing of order $\mathcal{O}(v^2/f^2)$ is introduced between B_H and W_H^3 through electroweak symmetry breaking, yielding

$$A_H = \cos \theta_H B_H - \sin \theta_H W_H^3, \quad M_{A_H}^2 = \frac{g'^2}{5} f^2 - \frac{g'^2}{4} v^2 + \mathcal{O}\left(\frac{v^4}{f^2}\right), \quad (13)$$

$$Z_H = \sin \theta_H B_H + \cos \theta_H W_H^3, \quad M_{Z_H}^2 = g^2 f^2 - \frac{g^2}{4} v^2 + \mathcal{O}\left(\frac{v^4}{f^2}\right), \quad (14)$$

$$\sin \theta_H = \frac{gg'}{4g^2 - \frac{4}{5}g'^2} \frac{v^2}{f^2} + \mathcal{O}\left(\frac{v^4}{f^4}\right), \quad (15)$$

and

$$W_H^\pm = (W_H^1 \mp W_H^2)/\sqrt{2}, \quad M_{W_H^\pm}^2 = g^2 f^2 - \frac{g^2}{4} v^2. \quad (16)$$

The A_H will be referred to as heavy photon throughout this text. It is always lighter than the other T-odd gauge bosons and thus a good candidate for the LTP (lightest T-odd particle)

and dark matter, if T-parity is an exact symmetry. Note that the mixing between the heavy photon and Z_H , is numerically small and leads to corrections at the 1% level at most.

In the scalar sector, T parity is defined as

$$\Pi \rightarrow -\Omega \Pi \Omega, \quad \Omega = \text{diag}(1, 1, -1, 1, 1), \quad (17)$$

such that H is T-even while Φ , ω and η are T-odd.

The kinetic term (2) is not the full non-linear sigma model Lagrangian but just the first term in an expansion in external momenta p . The higher order terms that have to be added to (2) to cancel divergencies that appear in perturbation theory are suppressed by powers of (p/Λ) , where Λ is the intrinsic cutoff of the theory beyond which ordinary perturbation theory breaks down.

In Little Higgs models $\Lambda = 4\pi f$ is typically of the order of 10 TeV, and the phenomenology at the TeV scale is well described by (2). Exceptions are possible if the lowest order Lagrangian possesses more symmetries than the full model. In that case higher order terms have to be taken into account and may change the phenomenology significantly.

T-parity also requires a doubling of the left-chiral fermion sector. Each left-handed T-even (SM) fermion is accompanied by a T-odd partner f_H (mirror fermion) with mass [13]

$$m_{f_{H,i}} = \sqrt{2}\kappa_i f + \mathcal{O}\left(\frac{v^2}{f}\right), \quad (18)$$

where the Yukawa couplings κ_i can in general depend on the fermion species i .

The implementation of the mass terms for the mirror fermions also introduces T-odd SU(2)-singlet fermions, which may receive large masses and do not mix with the SU(2)-doublets f_H . Here it is therefore assumed that these extra singlet fermions are too heavy to be observable at current or next-generation collider experiments.

The top sector requires an additional T-even fermion t'_+ and one T-odd fermion t'_- to cancel quadratic divergencies to the Higgs mass. Both particles obtain order f masses. We will not discuss the top sector of the Littlest Higgs model here, but refer the reader to Refs. [11,12] for further details. The Feynman rules of the Littlest Higgs model with T-parity are summarized in Ref. [12].

3 The WZW term in the Littlest Higgs model

3.1 The Wess Zumino Witten term

The nontrivial vacuum structure of the Littlest Higgs leads one to include the Wess Zumino Witten term [7] in the effective Lagrangian [5]. It consists of two parts,

$$\Gamma_{WZW} = \frac{N}{48\pi^2} (\Gamma_0(\Sigma) + \Gamma(\Sigma, A_l, A_r)). \quad (19)$$

Here Γ_0 is the ungauged WZW term that can be expressed as integral over a five-dimensional manifold with spacetime as its boundary [7], whereas $\Gamma(\Sigma, A_l, A_r)$ is the gauged part of the

WZW action that can be written as an ordinary four-dimensional spacetime integral. The explicit form of $\Gamma(\Sigma, A_l, A_r)$ and a prescription how to relate the gauge fields A_l, A_r to those appearing in the Littlest Higgs are given in Ref. [5]:

$$A_{l,r} = \sqrt{2}[g(W_L^a Q_L^a \mp W_H^a Q_H^a) + g'(B_L Y_L \mp B_H Y_H)]. \quad (20)$$

The Integer N depends on the UV completion of the Littlest Higgs model. In strongly coupled UV-completions, where the Little Higgs is a composite particle of some underlying Ultracolor theory [14], N will equal the number of ultracolors, $N = N_{uc}$.

The WZW term is T-odd by construction, i.e. it changes sign under a T-parity transformation. The fact that Γ_{WZW} violates T-parity and that its coefficient N can not be chosen arbitrarily make the WZW term stand out from other higher order terms in the expansion of the non-linear sigma model lagrangian.

In those cases where the UV completion demands a nonzero N , T-parity cannot be a fundamental symmetry of the full theory, instead it has to be seen as accidental symmetry of the lowest order effective Lagrangian. This is the point of view we want to adopt in this work.

3.2 Gauge invariance

The WZW term is not manifestly gauge invariant, rather under a gauge transformation

$$\Sigma \rightarrow e^{i\epsilon_l} \Sigma e^{-i\epsilon_r}, \quad A_l^\mu \rightarrow A_l^\mu + \partial^\mu \epsilon_l + i[\epsilon_l, A_l^\mu], \quad A_r^\mu \rightarrow A_r^\mu + \partial^\mu \epsilon_r + i[\epsilon_r, A_r^\mu], \quad (21)$$

it transforms as $\Gamma_{WZW} \rightarrow \Gamma_{WZW} + \delta\Gamma_{WZW}$, with $\delta\Gamma_{WZW}$ given by

$$\delta\Gamma_{WZW} = -\frac{N}{24\pi^2} \int d^4x \epsilon_{\mu\nu\rho\sigma} \text{Tr} [\epsilon_l (\partial^\mu A_l^\nu \partial^\rho A_l^\sigma - \frac{i}{2} \partial^\mu (A_l^\nu A_l^\rho A_l^\sigma)) - (L \rightarrow R)], \quad (22)$$

reproducing the well-known nonabelian chiral anomaly [7]. In order to restore gauge invariance, a sector must be added to the theory whose gauge variation cancels (22) exactly. Various options to cancel the anomaly are discussed in [6].

One possible way to cancel the anomaly directly at the level of the underlying ultracolor theory is by introducing a set of spectator leptons with $U(1)_1$ and $U(1)_2$ charges chosen such that they directly cancel the anomalies from the ultrafermions. Making the spectator leptons sufficiently heavy allows one to neglect their contributions to physical observables, without affecting the anomaly cancellation.

The anomalous couplings in Γ_{WZW} are the terms with three or four gauge bosons, with an odd number of T-odd gauge bosons. For example the three gauge boson terms with one T-odd gauge boson are of the form $\epsilon_{\mu\nu\rho\sigma} V_H^\mu V^\nu \partial^\rho V^\sigma$, where V_H is any T-odd gauge boson and V denote SM gauge bosons. Independent of the actual implementation, any anomaly canceling sector does at least cancel all these terms.

There could be additional effects from the anomaly canceling sector that do depend on the details of its implementation. We will here assume that these effects can be decoupled,

as in the example above, or at least are suppressed by some sufficiently large scale, and leave the details to further studies.

With the anomalous couplings cancelled, the leading T-odd interactions now appear at order $(1/f^2)$ in the expansion of Γ_{WZW} . For example three gauge boson interactions with two SM gauge bosons and one T-odd gauge boson are generated by $\epsilon_{\mu\nu\rho\sigma}H^\dagger H/f^2 V_H^\mu V^\nu \partial^\rho V^\sigma$ once electroweak symmetry is broken.

The systematic expansion of Γ_{WZW} leads to a large number of T-parity violating interactions. To leading order in $(1/f)$ the part of the WZW term containing one neutral T-odd gauge boson is given by

$$\Gamma_n = \frac{Ng^2g'}{48\pi^2f^2} \int d^4x (v+h)^2 \epsilon_{\mu\nu\rho\sigma} \times \quad (23)$$

$$\left[-\frac{6}{5}A_H^\mu (c_w^{-2}Z^\nu\partial^\rho Z^\sigma + W^{+\nu}D_A^\rho W^{-\sigma} + W^{-\nu}D_A^\rho W^{+\sigma} + i(3gc_w + g's_w)W^{+\nu}W^{-\rho}Z^\sigma) + \right.$$

$$\left. t_w^{-1}Z_H^\mu (2c_w^{-2}Z^\nu\partial^\rho Z^\sigma + W^{+\nu}D_A^\rho W^{-\sigma} + W^{-\nu}D_A^\rho W^{+\sigma} - 2i(2gc_w + g's_w)W^{+\nu}W^{-\rho}Z^\sigma) \right]$$

while the part containing one charged T-odd gauge boson reads

$$\Gamma_c = \frac{Ng^2g'}{48\pi^2f^2} \int d^4x (v+h)^2 \epsilon_{\mu\nu\rho\sigma} \times$$

$$\left[2W_H^{+\mu}W^{-\nu}(-c_w\partial^\rho A^\sigma + s_w\partial^\rho Z^\sigma) + c_w W_H^{+\mu}D_A^\nu W^{-\rho}(-A^\sigma + (2t_w + t_w^{-1})Z^\sigma) + \right.$$

$$\left. c_w D_A^\mu W_H^{+\nu}W^{-\rho}(A^\sigma + t_w^{-1}Z^\sigma) \right] + h.c., \quad (24)$$

written in unitary gauge. The vacuum expectation value of the Higgs field is denoted by v , h is the physical Higgs boson and we defined $D_A^\mu W^{\pm\nu} = (\partial^\mu \mp ieA^\mu)W^{\pm\nu}$. Furthermore s_w , c_w and t_w denote the sine, cosine and tangent of the weak mixing angle, respectively.

We do not write other parts of the WZW term here, instead all T-violating vertices with up to four legs have been tabulated in appendix B, including the interactions of the complex triplet Φ . These Feynman rules have further been implemented into a model file for CALCHEP 2.5 [15, 16].

Because of (23) the heavy photon can decay either into a pair of Z -bosons or into a W^+W^- pair, with a decay width of order $\mathcal{O}(\text{eV})$ [10]. This clearly rules out the A_H as dark matter candidate. A more detailed analysis, in particular for the case where the decay into real SM gauge bosons is kinematically forbidden, will be performed in section 4.

The gauge invariance of the WZW term can be verified using Ward identities for the three-point functions involving massive gauge bosons. These identities can be derived in a similar way as the Ward identities for three-boson vertices in the SM [17]. For example vertices involving the heavy photon A_H have to satisfy

$$k_2^\nu \Gamma_{\mu\nu\rho}^{A_H ZZ}(k_1, k_2, k_3) - im_Z \Gamma_{\mu\rho}^{A_H G^0 Z}(k_1, k_2, k_3) = 0, \quad (25)$$

$$k_2^\nu \Gamma_{\mu\nu\rho}^{A_H W^+ W^-}(k_1, k_2, k_3) - m_W \Gamma_{\mu\rho}^{A_H G^+ W^-}(k_1, k_2, k_3) = 0. \quad (26)$$

$$k_2^\nu \cdot \begin{array}{c} \text{---} A_{H,\mu}, k_1 \text{---} \\ \text{---} W_\nu^+, k_2 \text{---} \\ \text{---} W_\rho^-, k_3 \text{---} \end{array} - m_W \cdot \begin{array}{c} \text{---} A_{H,\mu}, k_1 \text{---} \\ \text{---} G^+, k_2 \text{---} \\ \text{---} W_\rho^-, k_3 \text{---} \end{array} = 0$$

Figure 1: Tree level Ward identity for the $A_H W^+ W^-$ vertex, all momenta incoming

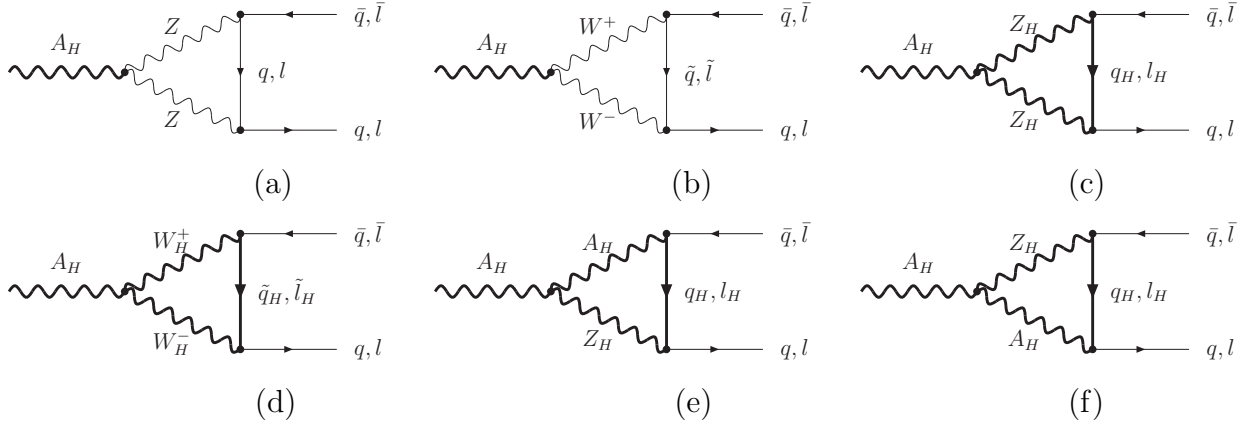


Figure 2: Loop induced decay of A_H into SM quarks/leptons. Thick lines indicate T-odd propagators. $q = (u, d, c, s, b)$, $\tilde{q} = (d, u, s, c, t)$, and similar for l, \tilde{l} .

At the tree level these identities have simple interpretations in terms of Feynman graphs, as shown in Fig. 1. Using the gauge boson-Goldstone boson vertices of Tab. 10 we have checked explicitly that $[SU(2) \times U(1)]_{SM}$ gauge invariance is respected by all interactions coming from equations (23) and (24).

3.3 Divergences and counterterms

Apart from the tree level interactions additional T-parity violating processes are induced at the loop level. These are especially important when corresponding tree level processes are kinematically forbidden. In particular, when $M_{A_H} < 2M_W$, the heavy photon cannot decay into real SM gauge bosons, and decays induced by one-loop processes have to be taken into account.

The most important processes are of the type shown in Fig. 2, where the heavy photon couples to two light T-even fermions via a triangle loop. A similar set of graphs also couple Z_H and W_H^\pm to SM fermions. Since the three-boson vertex involves one power of the loop momentum, graphs of this type are logarithmically divergent.

Particles	$c_{L,\epsilon}^f$	$c_{R,\epsilon}^f$
$A_H e^+ e^-$	$\frac{9\hat{N}}{160\pi^2} \frac{v^2}{f^2} g^4 g' (4 + (c_w^{-2} - 2t_w^2)^2)$	$-\frac{9\hat{N}}{40\pi^2} \frac{v^2}{f^2} g'^5$
$A_H \bar{\nu} \nu$	$\frac{9\hat{N}}{160\pi^2} \frac{v^2}{f^2} g^4 g' (4 + c_w^{-4})$	0
$A_H \bar{u}_a u_b$	$-\frac{\hat{N}}{160\pi^2} \frac{v^2}{f^2} g^4 g' (36 + (3c_w^{-2} - 4t_w^2)^2) \delta_{ab}$	$-\frac{\hat{N}}{10\pi^2} \frac{v^2}{f^2} g'^5 \delta_{ab}$
$A_H \bar{d}_a d_b$	$-\frac{\hat{N}}{160\pi^2} \frac{v^2}{f^2} g^4 g' (36 + (3c_w^{-2} - 2t_w^2)^2) \delta_{ab}$	$-\frac{\hat{N}}{40\pi^2} \frac{v^2}{f^2} g'^5 \delta_{ab}$

Table 1: Coefficients for the counterterm (27). Here $\hat{N} = \frac{N}{48\pi^2}$ denotes the coefficient of the WZW term, while a, b indicate the color indices of the external quarks.

The counterterms needed to cancel these divergencies are of the form

$$\mathcal{L}_{ct} = \bar{f} \gamma_\mu \left(c_L^f P_L + c_R^f P_R \right) f A_H^\mu, \quad (27)$$

$$c_i^f = c_{i,\epsilon}^f \left(\frac{1}{\epsilon} + \log \mu^2 + \mathcal{O}(1) \right). \quad (28)$$

The coefficients $c_i(\mu)$ of the counterterms are determined as follows. The scale dependence of the above loop processes must be cancelled by the scale dependence of the $c_i(\mu)$. Naturalness arguments then suggest that an $\mathcal{O}(1)$ change in the renormalization scale should be compensated by an $\mathcal{O}(1)$ change in the $c_i(\mu)$. Therefore these coefficients are given, up to $\mathcal{O}(1)$ factors, by the coefficients of the leading $1/\epsilon$ divergence in dimensional regularization of the above loop diagrams. The resulting coefficients are given in Tab. 1. Since the A_H only couples very weakly to fermions, the contributions of diagrams (e) and (f) in Fig. 2 have been neglected. An alternative, gauge invariant formulation of the counterterms (27) is discussed in appendix A.

Another important set of diagrams arises from those in Fig. 2 by replacing the A_H with a Z boson and one of the fermions with its mirror partner. These diagrams, as well as the corresponding diagrams where the Z is replaced by W^\pm , are again logarithmically divergent and require T-violating counterterms.² These may become important in scenarios where one of the mirror fermions is the LTP.

Other T-violating counterterms induced at the one loop level are not relevant for phenomenology for almost all reasonable choices of parameters in the Littlest Higgs model.

Mixing between T-even and T-odd gauge bosons is also induced by loop diagrams and may affect electroweak precision observables. The existing one loop graphs vanish due to the antisymmetry of the ϵ -tensor, so the first contributions come only at the two loop level. The nonvanishing two loop diagrams are shown in Fig. 3.

²The loop that couples the photon to a fermion-mirror fermion pair is finite, as required by gauge invariance.

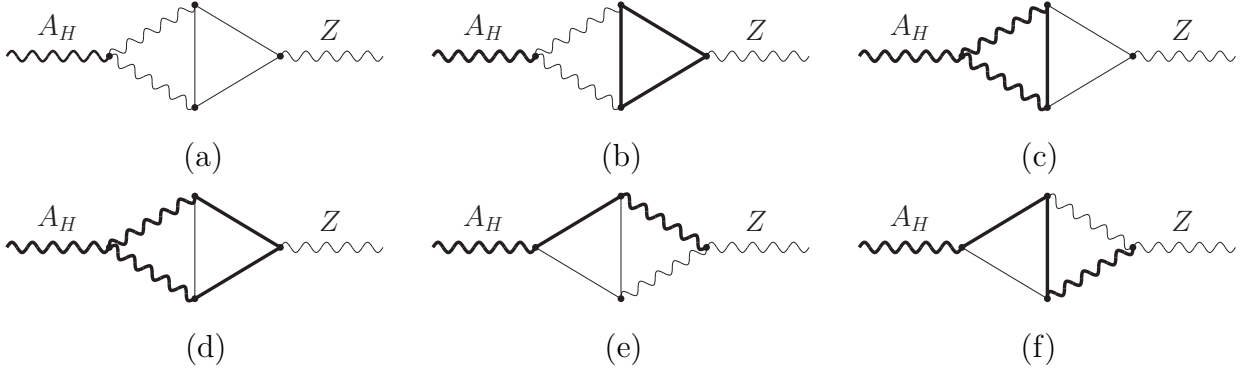


Figure 3: Two loop diagrams that contribute to A_H - Z boson mixing. As above thick lines indicate T -odd propagators. All types of fermions and mirror-fermions are allowed.

The relevant counterterms are of the form

$$\mathcal{L}_{ct} = \frac{c^{V_L V_H}}{4} (\partial_\mu V_{L,\nu} - \partial_\nu V_{L,\mu}) (\partial^\mu V_H^\nu - \partial^\nu V_H^\mu), \quad (29)$$

$$c^{V_L V_H} = c_\epsilon^{V_L V_H} \left(\frac{1}{\epsilon} + \log \mu^2 + \mathcal{O}(1) \right), \quad (30)$$

where $V_L \in \{A_L, Z_L, W_L^\pm\}$ and $V_H \in \{A_H, Z_H, W_H^\pm\}$. For the gauge boson mixing terms, the leading $1/\epsilon$ divergence is not completely determined in the LHT model. The reason is that the LHT model as a low-energy effective theory has an “incomplete” fermion content whose $[U(1)_i \times SU(2)_j \times SU(2)_j]$ gauge anomalies ($i, j = 1, 2$) must be cancelled (see above) by an interacting UV completion. If not specified, the $\mathcal{O}(1)$ uncertainty remains for the $1/\epsilon$ coefficients of the T -violating gauge boson mixing counterterms. For this reason we only list the parametric dependence of the coefficients $c_\epsilon^{V_L V_H}$ with an undetermined prefactor which is expected to be close to one:

$$c_\epsilon^{V_L V_H} = \text{const.} \times \frac{\hat{N}}{(4\pi)^4} \frac{v^2}{f^2} g^5 g' \left(B_0(k^2, 0, 0) + 2 \frac{m_t^2}{k^2} B_0(0, m_t^2, m_t^2) - (1 + 2 \frac{m_t^2}{k^2}) B_0(k^2, m_t^2, m_t^2) \right), \quad V_i = A_i, Z_i, \quad (31)$$

$$c_\epsilon^{W_L^\pm W_H^\pm} = \text{const.} \times \frac{\hat{N}}{(4\pi)^4} \frac{v^2}{f^2} g^5 g' \left(B_0(k^2, 0, 0) + \frac{m_t^2}{k^2} (1 - 2 \frac{m_t^2}{k^2}) B_0(0, 0, m_t^2) - \frac{(k^2 - m_t^2)(k^2 + 2m_t^2)}{k^4} B_0(k^2, 0, m_t^2) - \frac{m_t^2}{k^2} \right), \quad (32)$$

where all SM Yukawa couplings except the top Yukawa coupling have been set to zero, $\hat{N} = \frac{N}{48\pi^2}$ and “const.” stands for a complex $\mathcal{O}(1)$ constant, which depends on V_L and V_H . Here B_0 is the usual standard one-loop self-energy function and k is the external gauge boson momentum. The mixing between T -even and T -odd gauge bosons induced by the WZW term is very small due to the two-loop suppression and does not lead to observable effects in electroweak precision observables. For $m_t \rightarrow 0$ the gauge boson mixing terms have to vanish owing to gauge anomaly cancellation.

4 Phenomenology of T-parity breaking effects

4.1 Decays of A_H

The leading decays of A_H are induced by the $A_H W^+ W^-$ and $A_H Z Z$ terms in (23). For large enough f the decay into real gauge bosons is allowed and the corresponding partial widths are

$$\Gamma(A_H \rightarrow Z Z) = \frac{1}{2\pi} \left(\frac{N g'}{40\sqrt{3}\pi^2} \right)^2 \frac{m_{A_H}^3 m_Z^2}{f^4} \left(1 - \frac{4m_Z^2}{m_{A_H}^2} \right)^{\frac{5}{2}}, \quad (33)$$

$$\Gamma(A_H \rightarrow W^+ W^-) = \frac{1}{\pi} \left(\frac{N g'}{40\sqrt{3}\pi^2} \right)^2 \frac{m_{A_H}^3 m_W^2}{f^4} \left(1 - \frac{4m_W^2}{m_{A_H}^2} \right)^{\frac{5}{2}}. \quad (34)$$

To leading order in $(1/f)$ this agrees with the result of Ref. [10] if we set $K = 6\sqrt{5/3}$.

The threshold for the decay into real gauge bosons, $m_{A_H} > 2m_W$, corresponds to a value of $f = 1070$ GeV. However previous studies have shown that values of f as low as 500 GeV are consistent with electroweak precision data [11, 18]. In this region of parameter space, three-body decays via $A_H \rightarrow V V^*$ are dominant, where V^* indicates an off-shell SM gauge boson. For $f < 600$ GeV the mass of A_H even drops below M_W and four-body decays via two virtual intermediate gauge bosons have to be considered.

Below $f \sim 1200$ GeV the loop induced two body decays shown in Fig. 2 become relevant. A reliable estimate of the decay widths can be obtained by just using the finite, scale independent part of the counterterms and setting to one the undetermined $\mathcal{O}(1)$ coefficient that enters the results through the counterterms (27) (see section 3).

The partial width of a massive gauge boson V into a pair of fermions with couplings

$$\mathcal{L}_{Vff} = \bar{f} \gamma_\mu \left(\frac{r+l}{2} + \frac{r-l}{2} \gamma_5 \right) f V^\mu, \quad (35)$$

where l and r are the coefficients of the left and right chiral projectors, is given by

$$\Gamma_{V \rightarrow ff} = \frac{N_{C_f} M_V}{48\pi} \sqrt{1 - \frac{4m_f^2}{M_V^2}} \left[(r-l)^2 \left(1 - \frac{4m_f^2}{M_V^2} \right) + (r+l)^2 \left(1 + \frac{2m_f^2}{M_V^2} \right) \right], \quad (36)$$

N_{C_f} denoting the number of colors of fermion species f .

The total width of A_H for $N = 3$, including the loop induced two body decays, is shown in Fig. 4 together with the corresponding branching fractions. Above $f = 1500$ GeV, A_H dominantly decays into two on-shell gauge bosons, with a total width of $\Gamma_{A_H} \sim 1 - 2$ eV. The fermionic decay channels are negligible in this region.

Beneath the threshold for real W production, $M_{A_H} < 2m_W$, the decay phenomenology of A_H changes dramatically. For f below ~ 1000 GeV the decay into a light fermion pair becomes dominant; in approximately 10% of all cases, the decay is into a pair of charged leptons with an invariant mass m_{A_H} and an extremely small width of $\mathcal{O}(\text{eV})$.

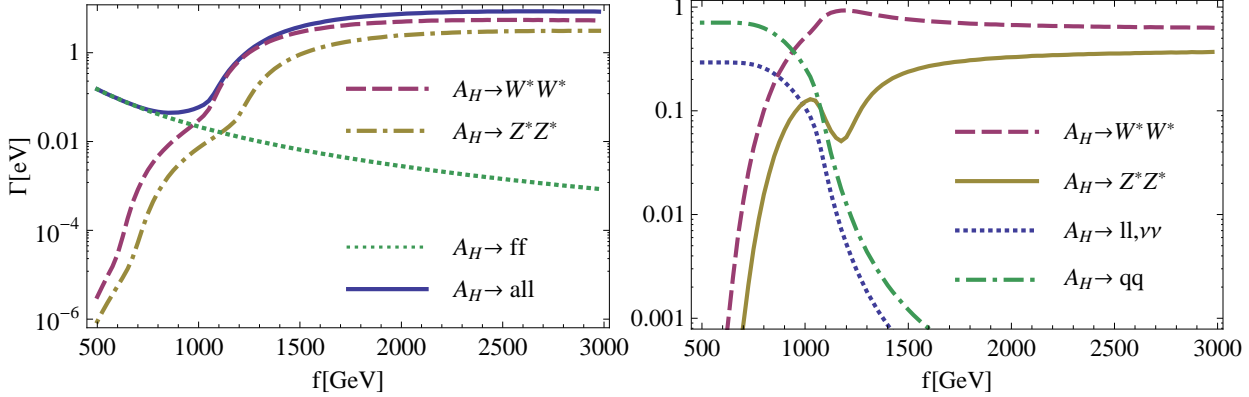


Figure 4: Left: Decay widths of A_H into Z^*Z^* (solid, red line), into W^*W^* (dashed, blue) and into fermion pairs (dotted, green) as well as the total width (thick black line), for $N = 3$. Right: Corresponding branching fractions. These are independent of N .

The uncertainty in the fermionic widths due to the unknown $\mathcal{O}(1)$ coefficients in the counterterms (27) may slightly change the value of f where the fermionic decays become dominant, however the overall picture does not change.

4.2 Bounds from electroweak precision tests and direct detection at LEP

T-parity in Little Higgs models evades the tension between a low value of f and electroweak precision tests (EWPT). Models without T-parity are typically only compatible with EWPT for $f \geq 5$ TeV [2], while lower values of f are favored by naturalness.

However, if T-parity is broken by the WZW term, the situation is different and we do not expect disagreement with electroweak precision data, even for values of f lower than 1 TeV. One reason is that the coefficient of Γ_{WZW} , $N/48\pi^2$, is very small for reasonable values of N . Furthermore, the T-odd operators affecting electroweak precision observables are suppressed by loops, as discussed in section 3, so that their contribution is smaller than the experimental error of those observables. We conclude that the Littlest Higgs model with anomalous T parity is not constrained by electroweak precision data; in particular values of f as low as 500 GeV are allowed. In addition the stringent bounds from dark matter overproduction are evaded.

While most of the T-odd particles are quite heavy, the A_H is rather light and could in principle have been produced and detected by the LEP experiments. However, the cross section for pair production of A_H in e^+e^- collisions is smaller than 10^{-6} pb for all allowed values of f , and thus invisible at LEP. T-violating single A_H production is further suppressed by $N/48\pi^2$ and therefore also out of reach of the LEP experiments.

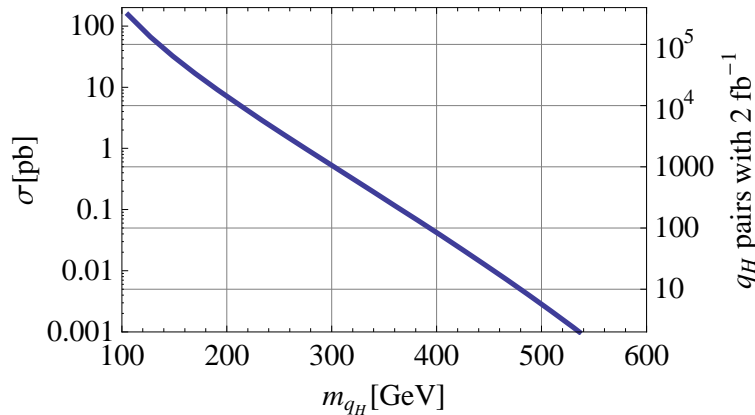


Figure 5: Cross section for first and second family mirror-quark pair production at Tevatron as a function of m_{q_H} . Right edge: Number of expected $q_H q_H$ pairs with 2 fb^{-1} of integrated luminosity.

4.3 Bounds from Tevatron

The rates for pair production of heavy gauge bosons are relatively small also at Tevatron. While the $A_H A_H$ production is suppressed due to its small couplings, other combinations like $A_H Z_H$ or $W_H^+ W_H^-$ are too heavy to be produced in noticeable amounts.

The situation is slightly different for the production of T-odd quark pairs. In the LHT, their mass is essentially a free parameter, only bound to lie between 100 GeV and a few TeV, so they can in principle be light enough to be produced in sizable amounts even at Tevatron.

The phenomenology of T-odd quarks at Tevatron has been studied in Ref. [19], assuming a common mass m_{q_H} for the first two families of T-odd quarks and exact T-parity. It was found that T-odd quarks are produced in sizeable numbers for $m_{q_H} < 500$ GeV and are excluded for $m_{q_H} < 350$ GeV in the $2j + \cancel{E}_T$ channel.³

After including the WZW term the collider signatures of a T-odd quark change completely. The main decay mode is still $q_H \rightarrow q A_H$, but the heavy photon A_H subsequently decays either into a pair of light fermions for small f or into a pair of (Standard Model) gauge bosons for larger values of f .

The cross section for the production of a $q_H \bar{q}_H$ pair in $p\bar{p}$ collisions depends strongly on their mass m_{q_H} and is nearly independent of f . It is therefore sufficient to analyse the phenomenology for two characteristic values of f , namely $f = 750$ GeV where A_H decays into fermion pairs in more than 90% of the cases, and $f = 1500$ GeV where essentially all A_H decay into gauge boson pairs. The results of this section furthermore do not depend on the actual value of N , as long as it is nonzero (see below).

The cross section for the pair production of mirror quarks at Tevatron is shown in Fig. 5, along with the number of expected $q_H q_H$ pairs produced with 2 fb^{-1} of integrated luminosity, as computed with CALCHEP. The renormalization and factorization scales μ were chosen

³For small T-odd masses m_{q_H} the dominant decay is $q_H \rightarrow q A_H$ which yields a $j + \cancel{E}_T$ signal if T-parity is unbroken.

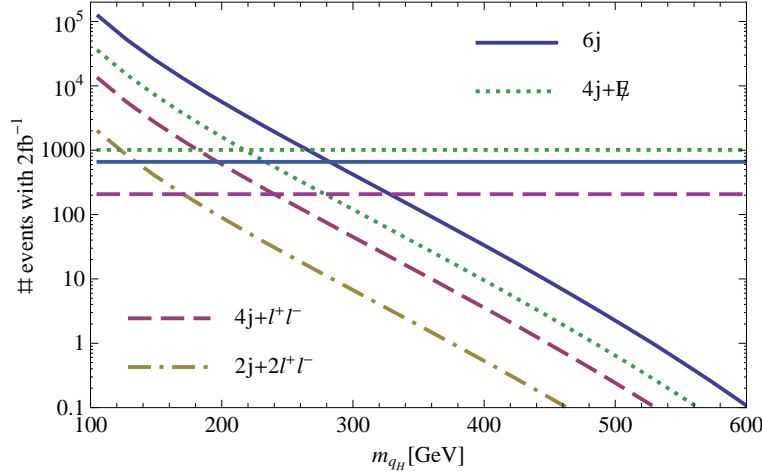


Figure 6: Event rates for the different decay channels of $q_H q_H$ pairs for $f = 750$ GeV with 2 fb^{-1} at Tevatron, together with the corresponding SM backgrounds (horizontal lines). No cuts have been applied to the signals.

to be the invariant mass of the incoming partons. This is a conservative choice as lower values of μ can increase the cross sections by up to 30%. To reduce this scale dependence a full next-to-leading order calculation of this process would be required.

We will first consider the case $f = 750$ GeV as a representative value for values of f below 1000 GeV, corresponding to A_H masses of 80–150 GeV. Here we assume that q_H is much heavier than A_H . The case where m_{q_H} is close to M_{A_H} is treated at the end of this section, while the case where (some of) the mirror fermions are lighter than A_H is discussed in section 4.5.

With A_H decaying, there are various possible final states originating from a $q_H \bar{q}_H$ pair. The highest rate results for the channel where both heavy photons decay into quark pairs, leading to six jets. Further there are events with four jets plus one lepton pair and events with two jets and two lepton pairs with the same invariant mass. Finally also four jets plus missing energy, two jets plus lepton pair plus missing energy and two jets plus missing energy are possible, since one or both A_H 's can decay into neutrinos. Figure 6 shows the expected number of events in the most promising channels together with the corresponding SM backgrounds (as listed in Ref. [20]) for 2 fb^{-1} , as a function of m_{q_H} . Note that we did not include detector acceptance effects in the computation of the signal, so that the experimentally observable rates could be slightly lower than the numbers in the figure.

The most stringent bounds on m_{q_H} could be derived from the six jet channel. Using the preliminary data from the CDF Vista global search [20] at 2 fb^{-1} we find that

$$m_{q_H} > 350 \text{ GeV}. \quad (37)$$

As mentioned, this bound could be improved by including NLO order corrections and appropriate cuts.

Due to their smaller background and cleaner signatures, the channels with leptonic final states could in principle provide stronger bounds than the one derived from purely hadronic

Final State	BF [%]	m_{q_H} [GeV]	Final State	BF [%]	m_{q_H} [GeV]
$8j + l + \nu_l$	22.5	335	$8j + l^+l^-$	4.4	270
$6j + 2(l\nu_l)$	13.9	315	$4j + 3l\nu_l$	4.1	265
$6j + 2(l^+l^-)$	0.4	185	$10j$	21.9	330

Table 2: Possible final states from the decay of a $q_H\bar{q}_H$ -pair for $f > 1000$ GeV, together with their branching fractions (second column) and the value of m_{q_H} where the expected number of events with 2 fb^{-1} at Tevatron drops below 100 (third column), assuming $B(A_H \rightarrow W^+W^-) = 66\%$. Here l denotes any of e, μ, τ .

decays. However in the interesting region above $m_{q_H} \gtrsim 300$ GeV their statistical significance drops quickly. A dedicated study of these final states still could yield more reliable the bounds, but this is not possible with the Vista data alone.

The analysis is more involved in the second case, $f > 1000$ GeV, where A_H dominantly decays into two gauge bosons. As can be seen in Fig. 4, or from equations (33) and (34), the branching $B(A_H \rightarrow W^+W^-)$ is larger than 60% in that region, with a peak value of $\sim 95\%$ around the W -boson pair production threshold.

The final states originating from the decay of a $q_H\bar{q}_H$ pair will consist of at least ten particles. Events with eight quarks and two leptons are the most common final state, followed by ten jet events and events with six quarks and four leptons in the final state. In most cases some or all of the leptons are neutrinos and escape detection, while the fraction of events where all leptons come in charged pairs is rather small.

To give an idea of the range of m_{q_H} that can be tested at Tevatron in this case, in Tab. 2 we list all final states with at least one charged lepton together with the value of m_{q_H} above which less than 100 events are to be expected with 2 fb^{-1} .

There are at least three channels where we expect a significant signal for $m_{q_H} < 300$ GeV, even after experimental cuts have been applied. The current data from Tevatron therefore strongly suggests that $m_{q_H} > 300$ GeV. It should be possible to derive more stringent bounds with a detailed analysis and refinement of some of the final states listed above. For instance, a fraction of the $6j + 2(l\nu_l)$ final state will have both leptons with the same-sign charge.

Finally we can discuss the case where q_H is only slightly heavier than A_H . This is possible only for somewhat larger values of f where we need to consider A_H decaying into SM gauge bosons. The quarks from the decay $q_H \rightarrow A_H + q$ are too soft to be observable in this case. Apart from this, the phenomenology is the same as in the previous analysis, in particular the results from Tab. 2 can be adopted by reducing the number of jets by two for each final state. With the same arguments as above we conclude that current experimental data strongly suggest $m_{q_H} > 300$ GeV also in this case.

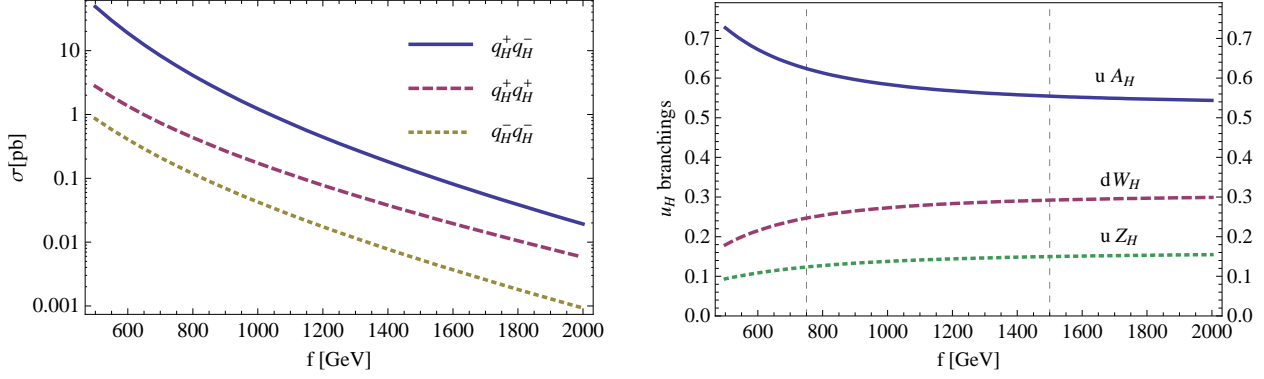


Figure 7: Left: Production of T-odd quark pairs, where $q^+ = \{u_H, \bar{d}_H, c_H, \bar{s}_H\}$ and $q^- = \{\bar{u}_H, d_H, \bar{c}_H, s_H\}$, as a function of f for $\kappa = 0.5$ Right: Branching fractions for the decay of u_H with $\kappa = 0.5$. The dashed vertical lines indicate our two reference scenarios with $f = 750$ GeV and $f = 1500$ GeV. The branching fractions for down-type mirror quarks d_H are similar, although there are small differences due to $\mathcal{O}(v^2/f^2)$ mass corrections [12, 23].

4.4 LHC phenomenology

Single production of T-odd particles is possible in principle at LHC, however the T-violating partial widths are too small for these processes to be observable. Therefore pair production remains the dominant source of T-odd particles. For LHC, the pair production rates, including the effects of the mirror fermions, have been studied in Refs. [21] and [22]. It turns out that not only the T-odd quark production but also the pair production rates for T-odd gauge bosons depend on the mass m_{q_H} of the mirror quarks.

For definiteness, we will take $\kappa = 0.5$ throughout this chapter and comment on other choices later. In this case the mirror quarks are always somewhat heavier than W_H and Z_H . As above we will consider two cases, case 1 with $f = 750$ GeV and case 2 with $f = 1500$ GeV. The corresponding particle masses are:

Case 1: $M_{W_H^\pm} = M_{Z_H} = 482$ GeV, $M_{A_H} = 111$ GeV, $m_{u_H} = 523$ GeV and $m_{d_H} = 530$ GeV for the first and second generation mirror quarks.

Case 2: $M_{W_H^\pm} = M_{Z_H} = 975$ GeV, $M_{A_H} = 235$ GeV, $m_{u_H} = 1057$ GeV and $m_{d_H} = 1061$ GeV for the first and second generation mirror quarks.

For the chosen value of κ the most important source of T-odd particles at LHC is the pair production of mirror quarks q_H . The left plot in Fig. 7 shows the cross sections for the production of equally charged and opposite charged mirror quark pairs, for the first two quark families. For moderate values of f the cross section for $q_H^+ q_H^-$ is of the order of one picobarn. The cross section for positively charged mirror quark pairs is larger than the one for quark pairs of negative charge and approaches the $q_H^+ q_H^-$ cross section for increasing values of f . As for the Tevatron calculation, the renormalization and factorization scales μ were chosen to be the invariant mass of the incoming partons. The scale uncertainty is again around 30%.

Signal rates for $f = 750$ GeV				
$q_H^+ q_H^- \rightarrow$	$q^+ q^- A_H A_H$ (BF: 39%)		$q^+ q^+ A_H W_H^-$ (BF: 15%)	
	Final State	$\sigma[\text{fb}]$	Final State	$\sigma[\text{fb}]$
	$6j$	994	$6j + l_*^- + \cancel{E}$	124
	$4j + \cancel{E}$	568	$4j + l_*^- + \cancel{E}$	71
	$4j + ll$	319	$4j + l_*^- + ll + \cancel{E}$	40
	$2j + 2ll$	26	$2j + l_*^- + 2ll + \cancel{E}$	3.2
$q_H^+ q_H^- \rightarrow$	$q^- q^+ W_H^- W_H^+$ (BF: 6%)		$q^+ q^- Z_H A_H$ (BF: 15%)	
	Final State	$\sigma[\text{fb}]$	Final State	$\sigma[\text{fb}]$
	$6j + l_*^+ l_*^- + \cancel{E}$	16.0	$6j + h$	306
	$4j + ll + l_*^+ l_*^- + \cancel{E}$	5.2	$4j + ll + h$	98
			$4j + h + \cancel{E}$	175

Table 3: Signal rates without cuts, from $q_H^+ q_H^-$ pair decays. Leptons $l = \{e, \mu, \tau\}$, and ll always denotes a charged lepton pair $l^+ l^-$ of the same flavor, while a hard charged lepton coming from a decay $W_H \rightarrow W A_H \rightarrow \nu l A_H$ is denoted by l_* .

The right plot in Fig. 7 shows the branching fractions for the two-body decays of an up-type mirror quark u_H as a function of f . While the decay into A_H and a SM quark dominates, the branching ratios for the other channels are sizeable, leading to a large variety of phenomenological signatures. Note that the mass of the mirror quarks always lies above the Tevatron bounds of section 4.3 for the considered range of parameters.

We will first discuss the signals stemming from the decay of opposite charge mirror quark pairs, $q_H^+ q_H^-$. When both q_H decay into $A_H + q$, the final states are the same as those discussed for Tevatron. The results for case 1 are shown in the upper left block of Tab. 3. The cross sections are large, in particular for the six jet channel, but also the channels with two or four charged leptons in the final states are well populated. For case 2 the cross sections, shown in Tab. 4, are significantly lower. A detailed analysis would be needed to extract a signal from the background in this case. However we expect very low SM background for the four-lepton channel, suggesting this signature as a promising discovery channel.

Consider now the case where one of the mirror quarks decays into $W_H + q$, and the other one into $A_H + q$. For the values of f considered here the branching fraction $B(W_H \rightarrow W A_H)$ is above 90% [10], so we will here neglect other decays. We then get

$$q_H^+ q_H^- \longrightarrow q^+ q^+ W^- A_H A_H \quad (38)$$

as intermediate decay product. We will focus on channels where the W^- decays leptonically,

Signal rates for $f = 1500$ GeV				
$q_H^+ q_H^- \rightarrow$	$q^+ q^- A_H A_H$ (BF: 31%)		$q^+ q^+ A_H W_H^-$ (BF: 16%)	
	Final State	$\sigma[\text{fb}]$	Final State	$\sigma[\text{fb}]$
	$10j$	8.2	$10j + l_*^- + \cancel{E}$	1.37
	$8j + l + \cancel{E}$	8.4	$8j + l_*^- + l + \cancel{E}$	1.40
	$6j + ll + \cancel{E}$	5.2	$8j + l_*^- + l^- + \cancel{E}$	0.70
	$6j + l^\pm l^\pm + \cancel{E}$	1.6	$l_*^- + ll + \cancel{E} + \text{jets}$	1.14
$q_H^+ q_H^- \rightarrow$	$q^- q^+ W_H^- W_H^+$ (BF: 9%)		$q^+ q^- Z_H A_H$ (BF: 17%)	
	Final State	$\sigma[\text{fb}]$	Final State	$\sigma[\text{fb}]$
	$10j + l_*^+ l_*^- + \cancel{E}$	0.25	$10j + h$	3.16
	$l_*^+ l_*^- + l + l + \cancel{E} + \text{jets}$	0.21	$6j + h + l^\pm l^\pm + \cancel{E}$	1.15

Table 4: Signal rates without cuts, from $q_H^+ q_H^-$ pair decays. Notation as in Tab. 3.

and denote the corresponding lepton by l_*^- . The results for both cases can be found in the upper right blocks of Tab. 3 and Tab. 4, respectively. For case 1, the interesting channels are the same as before, just with the l_*^- added. Since the W^- from the W_H decay is strongly boosted, a rather strong cut can be imposed on the transverse energy of l_*^- as well as on the missing transverse energy. This will effectively reduce the SM background, making these channels suitable for new physics searches, despite their somewhat smaller signal cross sections. Also for case 2 the cross sections are somewhat smaller than above. However due to the additional lepton, the same sign dilepton channel is enhanced, and furthermore the trilepton channel gets a sizeable cross section. In addition to the processes in the upper right block of Tab. 3 and Tab. 4 also the corresponding charge conjugate final states appear with the same cross sections. Combining both channels further increases the discovery reach in these decay modes.

Even more distinctive final states appear when both mirror quarks decay into $W_H + q$. Here we only consider channels where both W bosons originating from W_H 's decay leptonically. Thus every final state contains two oppositely charged leptons with uncorrelated flavor. For case 1 the cross sections are rather small compared to those of the channels considered above, so we only list the two strongest ones, in the lower left block of Tab. 3. Note that the channel with four leptons in the final state only has a slightly larger cross section than the five lepton channel from the $A_H W_H$ decay modes. We therefore do not expect these two channels to be particularly important for the discovery of the model. For case 2 the situation is similar. The cross sections for the two most interesting channels are shown in Tab. 4. The second channel has four uncorrelated leptons, and could for example

lead to $e^+e^+\mu^+\tau^-$ final states. While this channel is quite distinctive, it would require a higher luminosity than presently foreseen.

Finally we consider the case where the mirror quark pair decays into two quarks and $A_H Z_H$. The novel feature here is that Z_H decays into the Higgs boson and A_H with a branching fraction of $\sim 80\%$ [10]. We thus have processes of the form

$$q_H^+ q_H^- \longrightarrow q^+ q^- h A_H A_H. \quad (39)$$

The actual value of $B(Z_H \rightarrow h A_H)$ depends on the Higgs boson mass, but lies above $\sim 80\%$ as long as the Z_H is somewhat heavier than the decay products, i.e. $M_{Z_H} > m_h + M_{A_H}$. The number of Higgs bosons produced in this channel can be sizeable as illustrated in Tab. 3 and Tab. 4, respectively. Depending on the Higgs boson mass, the (very) final states vary and a more detailed analysis would be required if a signal would surface. In Tab. 3 we list the three channels with the largest cross section. The production rates for $h + \text{jets}$ and for $h + \text{jets} + \cancel{E}$ are sizeable, in total around 0.5 pb. This is similar to $t\bar{t}h$ production in the SM, especially for larger values of the Higgs mass. The channel with a charged lepton pair produced along with the Higgs boson is particularly interesting. The signal is comparable to the SM background coming from Zh production, but can be distinguished by requiring additional jets from the q_H decays and by the fact that the lepton pair has an invariant mass M_{A_H} .

As expected, the cross sections are much smaller for case 2. We were still able to identify an interesting channel where the Higgs is produced along with two equally charged leptons. While the signal is rather small, the same is true for the SM background. The results for this channel and for $h + 10$ jets production are shown in the lower right block of Tab. 4.

Next we will discuss the signals from decays of positively charged mirror quark pairs, $q_H^+ q_H^+$. Since the production rate for same sign mirror quark pairs is almost one order of magnitude smaller than the one for opposite sign mirror quarks, we will only consider decay modes that lead to a distinctive final state. These mainly come from processes where both mirror quarks decay into W_H^+ and a quark, leading to

$$q_H^+ q_H^+ \longrightarrow q^- q^- W^+ W^+ A_H A_H. \quad (40)$$

To be sensitive to the charges we only consider leptonic decays of the W bosons, leading to two positively charged hard leptons which we will again denote by l_*^+ .

The signal rates for both case 1 and case 2 can be found in Tab. 5. Since we require leptonic decays of at least two W bosons, the signal rates for both cases are rather small. With suitable cuts on the transverse momentum of the two hard leptons it should still be possible to efficiently remove the SM background.

T-odd gauge bosons in general provide a cleaner signature, since less particles are produced in their decay. However the cross section for T-odd gauge boson pair production is rather small. For the values of f and κ chosen here at least ten times more T-odd gauge bosons are produced in the decays of mirror quarks.

Same Sign Multilepton Rates			
$f = 750 \text{ GeV}$		$f = 1500 \text{ GeV}$	
Final State	$\sigma[\text{fb}]$	Final State	$\sigma[\text{fb}]$
$6j + l_*^+ l_*^+$	1.56	$l_*^+ l_*^+ + \text{anything}$	0.256
$4j + l_*^+ l_*^+ + \cancel{E}$	0.89	$l_*^+ l_*^+ + l^+ + \text{anything}$	0.115
$4j + l_*^+ l_*^+ + ll$	0.50		

Table 5: Rates for same sign lepton signals, from $q_H^+ q_H^+$ pair decays. Notation as in Tab. 3 and “anything” stands for additional jets, leptons and/or missing energy from neutrinos.

Furthermore it is hard to distinguish directly produced T-odd gauge bosons from those coming from mirror quark decays. The reason is that while the possible final states differ in the total number of jets, that number is rather large for most processes and thus would require a full reconstruction of all events to be measured.

A comment on the effects of a variation of the free parameters is in order. If f is increased further, all T-odd particle masses are increased and the cross sections for all processes go down, while the final states and their branching fractions remain essentially unchanged.

Changing κ , on the contrary, changes the results more significantly because it affects the mirror quark mass m_{q_H} while leaving the heavy gauge boson masses unchanged. If κ goes below 0.45, the decays into most T-odd gauge bosons become inaccessible, leaving $A_H + q$ as the only two-body final state. In that case direct T-odd gauge boson pair production becomes important, since W_H and Z_H are not obtained from q_H decays anymore. The extreme case where the mirror quarks are also lighter than A_H will be discussed in the next chapter. On the other hand, if κ is increased, the cross section for $q_H q_H$ pair production decreases while at the same time most cross sections for T-odd gauge boson pair production increase, as has been shown in [21]. A further effect is that the branching fractions of q_H change, with the branching fraction $B(q_H \rightarrow q W_H)$ reaching around 60%, while $B(q_H \rightarrow q A_H)$ drops below the 10% level.

The T-odd gauge boson pair production rates are affected differently by increasing κ . While the cross section for $pp \rightarrow W_H^+ Z_H$ increases, the one for $pp \rightarrow W_H^+ A_H$ is reduced [21]. If the mirror quarks are very heavy and only the T-odd gauge bosons are accessible, the ratio of these cross sections provides a possibility to measure m_{q_H} indirectly.

While inclusion of the WZW term leads to many new signatures of the Littlest Higgs model at LHC, none of the processes discussed above is actually sensitive to its integer parameter N . The reason is that vertices containing the WZW term only appear in decays, and all partial width are multiplied by the same power of N . Measuring the total width of A_H could in principle give access to N , however in practice a width of the order of one eV is

not measurable. The same problem appears if one tries to measure the T-violating partial widths in the decays of other T-odd particles like W_H . T-violating decays into two gauge bosons can be distinguished from T-conserving decays by measuring the distribution of the angle between the outgoing gauge bosons and the polarization axis of W_H [8]. In practice however the T-violating partial width is too small for this analysis to be feasible.

Single T-odd gauge boson production via gauge boson fusion would give direct access to N . This process is not in the reach of LHC, but might be detectable at a very luminous linear collider.

4.5 The Case of a fermionic LTOP

The masses of the mirror fermions are free parameters in the LHT, determined by the parameters κ_i . Thus in principle some of them could be lighter than the lightest T-odd gauge boson A_H . With T-parity broken these fermions are unstable, so any of them could be the lightest T-odd particle (LTOP).

Since the WZW term breaks T-parity directly only in the gauge sector, the simplest decay process is a three body decay mediated by a virtual T-odd gauge boson. Loop induced two body decays can be of similar importance. The most relevant diagrams are similar to those shown in Fig. 2, with the A_H replaced by a Z or W boson and one of the external fermions replaced by the fermionic LTOP f_H . Major decay channels therefore are $f_H \rightarrow Zf$, $f_H \rightarrow W\tilde{f}$ and $f_H \rightarrow A_H^*f$. The last channel will either yield a three fermion final state $f'\tilde{f}'f$ or a VVf final state with two SM gauge bosons, depending on the mass of f_H and A_H and the kinematics of the decay.

We will now briefly discuss how this could affect the phenomenology at hadron colliders. If f_H is a T-odd quark, it will be pair produced directly in sizeable amounts and decay as discussed above. Furthermore most of the directly produced T-odd gauge bosons will decay into $f_H f$ pairs, since the direct decay into SM particles via the WZW term is suppressed in general. If the mirror quark masses are somewhat hierarchical, one could also imagine longer decay chains, with the branching fractions depending on the flavor structure of the mirror quark sector.

Even more appealing is the case where f_H is a lepton. While their direct production rate is small in that case, the pair produced mirror quarks will now decay via long chains:

$$q_H \longrightarrow A_H q \longrightarrow l_H^\pm l^\mp q \longrightarrow \dots, \quad (41)$$

$$q_H \longrightarrow W_H q \longrightarrow A_H W q \longrightarrow l_H^\pm f^\mp W q \longrightarrow \dots \quad (42)$$

Studying these novel collider signatures of the Littlest Higgs model in more detail would certainly be interesting.

5 Conclusion

In this paper we have considered some phenomenological consequences of the natural T-parity breaking Wess-Zumino-Witten term in the effective Lagrangian of the classically T-parity invariant Littlest Higgs model. In particular we have calculated the loop induced

decays of the heavy photon A_H into normal fermion pairs, assuming A_H to be the lightest T-odd particle. These complement the known tree level decays into normal gauge bosons [10] and are the dominant modes for breaking scales below 1 TeV. For these values, the effect is quite distinct and changes the phenomenology of the model substantially, because A_H appears as a decay product of any other T-odd particle. Due to its small prefactor the Wess-Zumino-Witten term only makes a negligible contribution to electroweak precision observables.

The new decay modes typically give rise to final states with many jets. Comparing with published data from other new physics searches at the Tevatron, this leads to improved bounds on the mass of the heavy quarks q_H for values of the breaking scale below 1 TeV. If q_H is heavier than A_H , the new decays of the latter induce new decays of q_H . In particular, as illustrated in Figure 6, six jet events give rise to a quite strict limit on m_{q_H} of 350 GeV for $f = 750$ GeV. But the present study gives only a rough picture and a refined analysis would be necessary for more accurate results.

At the LHC, the situation is even better. For $q_H \bar{q}_H$ pairs, their decays into light quarks (antiquarks) and A_H would lead to the same final states as discussed above. But because of the higher energy, larger heavy quark masses can be probed, where decays of the form $q_H \rightarrow q + W_H$ are possible, leading to very distinctive final states which may be distinguished from SM background. Of particular interest in this respect are final states with four leptons. Even more tantalizing are processes involving a Z_H boson decaying through a Higgs boson. The production rate for h +jets (and missing energy) from these processes is sizeable, possibly comparable to the SM top associated Higgs boson production rate, although highly dependent on f and the masses m_{q_H} . For a moderately heavy Higgs ($m_h \sim 200$ GeV), and a mirror mass around $m_{q_H} \sim 350 - 400$ GeV as well as $f \sim 500$ GeV, the production rate can be of the order of 10 pb or more. This is important since other Higgs production channels are reduced in the Littlest Higgs model [24]. The production of two equally charged heavy particles, $q_H^\pm q_H^\pm$, is possible, yielding striking same-sign lepton signatures but small rates.

In this work we have not considered associated production of heavy quarks with heavy gauge bosons and production of the top quark partners, since pair production of first generation heavy quarks has a substantially larger cross section and thus is more suitable for a first new physics discovery. Nevertheless, a detailed analysis of those processes would be interesting for future work since they could reveal additional information about the model structure.

Because of the small T-violating branching ratios, singly produced T-odd particles are practically non-observable and thus only pair production is phenomenologically relevant.

Finally we have also considered the case of a fermionic lightest T-odd particle. This would lead to still different signatures that will have to be worked out in detail.

Acknowledgments

PS wants to thank N. Greiner and Z. Kunszt for useful discussions. AF is grateful to Argonne National Laboratory, the University of Chicago and the Universität Zürich for hospitality during stages of this work. This work was supported in part by the Schweizer Nationalfonds.

Note added: Recently W. Keung, I. Low and J. Shu [29] proposed a method to distinguish WZW-term induced decays of heavy gauge bosons from decays mediated by other operators. For large enough f this method can be used to analyse the $A_H \rightarrow ZZ$ decay at LHC.

A T-odd gauge invariant counterterms

The counterterms (27) introduced in section 3 are not invariant under the global symmetries or gauge transformations because they were constructed to cancel divergencies in particular diagrams. In general, couplings between heavy gauge bosons and SM fermions cannot be written as covariant derivatives in a fermionic kinetic term. Similarly, counterterms involving T-odd gauge bosons as well as the massive standard model gauge bosons also need to be present; again they do not surface in a symmetric way at first. We note however that the simple counterterms in (27) are only required to cancel divergencies affecting broken gauge symmetries and thus no $U(1)_{em}$ breaking counterterms are required.

As is well known in chiral perturbation theory, one can do better and construct directly the required symmetric counterterms, [25]. Also in the present case we can rewrite the counterterms in a form that preserves gauge invariance and furthermore reflect the underlying $SU(5)$ symmetric structure of the models. The point is to insert the non-linear sigma model field Σ into the covariant derivative for the fermions, to define objects with well-defined transformations properties, such as vectorial and axial currents and consider appropriate powers of them. We do not give a systematic exposition here but refer to a future publication. For the purely mesonic WZW term, such a complete analysis was given in [26].

As illustration of the procedure, the counterterms for the diagram in Fig. 2 (b) could have contributions from a term

$$c_{ct} \bar{f} Q_W^2 (\Sigma^\dagger D_\mu \Sigma - \Sigma D_\mu \Sigma^\dagger) \gamma^\mu P_L f. \quad (43)$$

Here $f = (\psi_1, 0, \psi_2)^T$ contains the lefthanded fermion doublets ψ_1 and ψ_2 that yield the lefthanded SM fermions $\psi_{SM} = \frac{1}{\sqrt{2}}(\psi_1 - \psi_2)$ as well as their mirror partners $\psi_H = \frac{1}{\sqrt{2}}(\psi_1 + \psi_2)$. The 5×5 matrix Q_W is defined as $Q_W = Q^+ + Q^-$, where Q^+ and Q^- are the generators of the W^+ and W^- bosons that run in the loop, and c_{ct} is an appropriate coefficient for the counterterm.

This term is gauge invariant. Upon electroweak symmetry breaking it generates counterterms at order v^2/f^2 as required to match the results of Tab. 1. The righthanded fermions are gauge singlets, so their counterterms have to be generated differently. A possible term is

$$c_{ct} \bar{f} \gamma^\mu P_R f \text{Tr} [Q_W^2 (\Sigma^\dagger D_\mu \Sigma - \Sigma D_\mu \Sigma^\dagger)]. \quad (44)$$

Counterterms of this form were introduced in [27] where they are used to regularize the divergencies in the loop induced decay of the neutral pion π^0 into lepton pairs, a process that is similar to the decay of A_H into lepton pairs as discussed in section 3.

B Feynman rules for the LHT with WZW term

The Feynman rules for the original Littlest Higgs model are listed in Ref. [28]. An almost complete collection (to leading order in $1/f$) of Feynman rules for the Littlest Higgs model with T-parity, including flavor effects, can be found in Ref. [12].

In Tabs. 6–13 we provide the additional Feynman rules introduced by the WZW term after anomaly cancellation, to leading order in $(1/f)$. The small mixing between A_H and Z_H is neglected since it is numerically less important than other subleading $(1/f)$ corrections.

We use the conventions of Ref. [30] with all momenta incoming. The Feynman rules can be translated to CalcHEP conventions by multiplying each vertex with $(-i)$ and changing $p_i^\mu \rightarrow -p_i^\mu$ for all momenta in the vertex. We work in a general covariant gauge. An overall factor $\hat{N} = \frac{N}{48\pi^2}$ has been factored out from all the Feynman rules. Vertices that are zero have been omitted.

Particles			Vertices
$A_{H\mu}$	W_ν^+	W_ρ^-	$-\frac{6}{5} \frac{e^3 v^2}{c_w s_w^2 f^2} \varepsilon_{\mu\nu\rho\sigma} (p_2^\sigma - p_3^\sigma)$
$A_{H\mu}$	Z_ν	Z_ρ	$-\frac{6}{5} \frac{e^3 v^2}{c_w s_w^2 f^2} \varepsilon_{\mu\nu\rho\sigma} (p_2^\sigma - p_3^\sigma)$
A_μ	W_ν^+	$W_{H\rho}^-$	$\frac{e^3 v^2}{s_w^2 f^2} \varepsilon_{\mu\nu\rho\sigma} (p_2^\sigma + p_3^\sigma - 2p_1^\sigma)$
A_μ	W_ν^-	$W_{H\rho}^+$	$\frac{e^3 v^2}{s_w^2 f^2} \varepsilon_{\mu\nu\rho\sigma} (p_3^\sigma + p_2^\sigma - 2p_1^\sigma)$
$A_{H\mu}$	$A_{H\nu}$	$Z_{H\rho}$	$-\frac{4}{5} \frac{e^3 v^2}{c_w^2 s_w f^2} \varepsilon_{\mu\nu\rho\sigma} (p_1^\sigma - p_2^\sigma)$
$A_{H\mu}$	$W_{H\nu}^+$	$W_{H\rho}^-$	$-\frac{4}{5} \frac{e^3 v^2}{c_w s_w^2 f^2} \varepsilon_{\mu\nu\rho\sigma} (p_2^\sigma - p_3^\sigma)$
$A_{H\mu}$	$Z_{H\nu}$	$Z_{H\rho}$	$\frac{4}{5} \frac{e^3 v^2}{c_w s_w^2 f^2} \varepsilon_{\mu\nu\rho\sigma} (p_3^\sigma - p_2^\sigma)$
W_μ^+	W_ν^-	$Z_{H\rho}$	$-\frac{e^3 v^2}{s_w^3 f^2} \varepsilon_{\mu\nu\rho\sigma} (p_2^\sigma - p_1^\sigma)$
W_μ^+	$W_{H\nu}^-$	Z_ρ	$-\frac{e^3 v^2}{c_w s_w^3 f^2} \varepsilon_{\mu\nu\rho\sigma} ((1 + s_w^2)p_1^\sigma - 2s_w^2 p_3^\sigma - c_w^2 p_2^\sigma)$
W_μ^-	$W_{H\nu}^+$	Z_ρ	$\frac{e^3 v^2}{c_w s_w^3 f^2} \varepsilon_{\mu\nu\rho\sigma} (c_w^2 p_2^\sigma + 2s_w^2 p_3^\sigma - (1 + s_w^2)p_1^\sigma)$
$W_{H\mu}^+$	$W_{H\nu}^-$	$Z_{H\rho}$	$\frac{e^3 v^2}{s_w^3 f^2} \varepsilon_{\mu\nu\rho\sigma} (p_1^\sigma - p_2^\sigma)$
Z_μ	Z_ν	$Z_{H\rho}$	$-2 \frac{e^3 v^2}{c_w^2 s_w^3 f^2} \varepsilon_{\mu\nu\rho\sigma} (p_2^\sigma - p_1^\sigma)$

Table 6: T-parity violating three gauge boson vertices. The momenta $p_{1,2,3}$ correspond to the particle in the first, second, and third column, respectively.

Particles				Vertices
A_μ	$A_{H\nu}$	W_ρ^+	W_σ^-	$\frac{12}{5} \frac{e^4 v^2}{c_w s_w^2 f^2} \varepsilon_{\mu\nu\rho\sigma}$
A_μ	$A_{H\nu}$	$W_{H\rho}^+$	$W_{H\sigma}^-$	$\frac{8}{5} \frac{e^4 v^2}{c_w s_w^2 f^2} \varepsilon_{\mu\nu\rho\sigma}$
A_μ	W_ν^+	W_ρ^-	$Z_{H\sigma}$	$-2 \frac{e^4 v^2}{s_w^3 f^2} \varepsilon_{\mu\nu\rho\sigma}$
A_μ	W_ν^+	$W_{H\rho}^-$	Z_σ	$2 \frac{e^4 v^2}{c_w s_w^3 f^2} \varepsilon_{\mu\nu\rho\sigma}$
A_μ	W_ν^-	$W_{H\rho}^+$	Z_σ	$-2 \frac{e^4 v^2}{c_w s_w^3 f^2} \varepsilon_{\mu\nu\rho\sigma}$
A_μ	$W_{H\nu}^+$	$W_{H\rho}^-$	$Z_{H\sigma}$	$-2 \frac{e^4 v^2}{s_w^3 f^2} \varepsilon_{\mu\nu\rho\sigma}$
$A_{H\mu}$	W_ν^+	W_ρ^-	Z_σ	$-\frac{6}{5} \frac{(3-2s_w^2)e^4 v^2}{c_w^2 s_w^3 f^2} \varepsilon_{\mu\nu\rho\sigma}$
$A_{H\mu}$	W_ν^+	$W_{H\rho}^-$	$Z_{H\sigma}$	$-\frac{4}{5} \frac{e^4 v^2}{c_w s_w^3 f^2} \varepsilon_{\mu\nu\rho\sigma}$
$A_{H\mu}$	W_ν^-	$W_{H\rho}^+$	$Z_{H\sigma}$	$\frac{4}{5} \frac{e^4 v^2}{c_w s_w^3 f^2} \varepsilon_{\mu\nu\rho\sigma}$
$A_{H\mu}$	$W_{H\nu}^+$	$W_{H\rho}^-$	Z_σ	$-\frac{4}{5} \frac{(1-2s_w^2)e^4 v^2}{c_w^2 s_w^3 f^2} \varepsilon_{\mu\nu\rho\sigma}$
W_μ^+	W_ν^-	Z_ρ	$Z_{H\sigma}$	$-2 \frac{(2-s_w^2)e^4 v^2}{c_w s_w^4 f^2} \varepsilon_{\mu\nu\rho\sigma}$
$W_{H\mu}^+$	$W_{H\nu}^-$	Z_ρ	$Z_{H\sigma}$	$-2 \frac{c_w e^4 v^2}{s_w^4 f^2} \varepsilon_{\mu\nu\rho\sigma}$

Table 7: *T*-parity violating vertices with four gauge bosons.

Particles			Vertices
W_μ^+	$W_{H\nu}^-$	h	$\frac{e^2 v}{s_w^2 f^2} \varepsilon_{\mu\nu\rho\sigma} (p_2^\rho - p_1^\rho) p_3^\sigma$
W_μ^-	$W_{H\nu}^+$	h	$\frac{e^2 v}{s_w^2 f^2} \varepsilon_{\mu\nu\rho\sigma} (p_1^\rho - p_2^\rho) p_3^\sigma$

Table 8: *T*-parity violating vertices with one physical scalar and two gauge bosons. The momenta $p_{1,2,3}$ correspond to the particle in the first, second, and third column, respectively.

Particles				Vertices
A_μ	W_ν^+	$W_{H\rho}^-$	h	$2 - \frac{e^3 v}{s_w^2 f^2} \varepsilon_{\mu\nu\rho\sigma} (p_2^\sigma + p_3^\sigma - 2p_1^\sigma)$
A_μ	W_ν^-	$W_{H\rho}^+$	h	$-2 \frac{e^3 v}{s_w^2 f^2} \varepsilon_{\mu\nu\rho\sigma} (p_3^\sigma + p_2^\sigma - 2p_1^\sigma)$
$A_{H\mu}$	$A_{H\nu}$	$Z_{H\rho}$	h	$\frac{8}{5} \frac{e^3 v}{c_w^2 s_w f^2} \varepsilon_{\mu\nu\rho\sigma} (p_1^\sigma - p_2^\sigma)$
$A_{H\mu}$	W_ν^+	W_ρ^-	h	$\frac{12}{5} \frac{e^3 v}{c_w s_w^2 f^2} \varepsilon_{\mu\nu\rho\sigma} (p_2^\sigma - p_3^\sigma)$
$A_{H\mu}$	$W_{H\nu}^+$	$W_{H\rho}^-$	h	$\frac{8}{5} \frac{e^3 v}{c_w s_w^2 f^2} \varepsilon_{\mu\nu\rho\sigma} (p_2^\sigma - p_3^\sigma)$
$A_{H\mu}$	Z_ν	Z_ρ	h	$-\frac{12}{5} \frac{e^3 v}{c_w^3 s_w^2 f^2} \varepsilon_{\mu\nu\rho\sigma} (p_3^\sigma - p_2^\sigma)$
$A_{H\mu}$	$Z_{H\nu}$	$Z_{H\rho}$	h	$\frac{8}{5} \frac{e^3 v}{c_w s_w^2 f^2} \varepsilon_{\mu\nu\rho\sigma} (p_2^\sigma - p_3^\sigma)$
W_μ^+	W_ν^-	$Z_{H\rho}$	h	$2 \frac{e^3 v}{s_w^3 f^2} \varepsilon_{\mu\nu\rho\sigma} (p_2^\sigma - p_1^\sigma)$
W_μ^+	$W_{H\nu}^-$	Z_ρ	h	$2 \frac{e^3 v}{c_w s_w^3 f^2} \varepsilon_{\mu\nu\rho\sigma} ((1 + s_w^2) p_1^\sigma - 2s_w^2 p_3^\sigma - c_w^2 p_2^\sigma)$
W_μ^-	$W_{H\nu}^+$	Z_ρ	h	$-2 \frac{e^3 v}{c_w s_w^3 f^2} \varepsilon_{\mu\nu\rho\sigma} (c_w^2 p_2^\sigma + 2s_w^2 p_3^\sigma - (1 + s_w^2) p_1^\sigma)$
$W_{H\mu}^+$	$W_{H\nu}^-$	$Z_{H\rho}$	h	$-2 \frac{e^3 v}{s_w^3 f^2} \varepsilon_{\mu\nu\rho\sigma} (p_1^\sigma - p_2^\sigma)$
Z_μ	Z_ν	$Z_{H\rho}$	h	$4 \frac{e^3 v}{c_w^2 s_w^3 f^2} \varepsilon_{\mu\nu\rho\sigma} (p_2^\sigma - p_1^\sigma)$

Table 9: T -parity violating vertices with one physical scalar and three gauge bosons. The momenta $p_{1,2,3,4}$ correspond to the particle in the first, second, third and fourth column, respectively.

Particles				Vertices
$A_{H\mu}$	W_ν^\pm	G^\mp		$\mp \frac{6}{5} \frac{e^2 v}{c_w s_w f^2} \varepsilon_{\mu\nu\rho\sigma} p_3^\rho (p_1^\sigma - p_2^\sigma)$
$A_{H\mu}$	Z_ν	G^0		$-\frac{6}{5} \frac{ie^2 v}{c_w^2 s_w f^2} \varepsilon_{\mu\nu\rho\sigma} p_3^\rho (p_1^\sigma - p_2^\sigma)$
$W_{H\mu}^\pm$	A_ν	G^\mp		$\mp 3 \frac{e^2 v}{s_w f^2} \varepsilon_{\mu\nu\rho\sigma} p_3^\rho (p_1^\sigma - p_2^\sigma)$
$Z_{H\mu}$	W_ν^\pm	G^\mp		$\pm \frac{e^2 v}{s_w^2 f^2} \varepsilon_{\mu\nu\rho\sigma} p_3^\rho (p_1^\sigma - p_2^\sigma)$
$W_{H\mu}^\pm$	Z_ν	G^\mp		$\mp \frac{e^2 (c_w^2 - 2s_w^2) v}{c_w s_w^2 f^2} \varepsilon_{\mu\nu\rho\sigma} p_3^\rho (p_1^\sigma - p_2^\sigma)$
$W_{H\mu}^\pm$	W_ν^\pm	G^0		$2 \frac{ie^2 v}{s_w^2 f^2} \varepsilon_{\mu\nu\rho\sigma} p_3^\rho (p_1^\sigma - p_2^\sigma)$
$Z_{H\mu}$	Z_ν	G^0		$2 \frac{ie^2 v}{c_w s_w^2 f^2} \varepsilon_{\mu\nu\rho\sigma} p_3^\rho (p_1^\sigma - p_2^\sigma)$

Table 10: T -parity violating vertices with one SM Goldstone and two gauge bosons. The momenta $p_{1,2,3}$ correspond to the particle in the first, second, and third column, respectively.

Particles				Vertices
A_μ	$A_{H\nu}$	Φ^+	Φ^-	$\frac{2}{5} \frac{e^2}{c_w f^2} \varepsilon_{\mu\nu\rho\sigma} (p_1^\rho p_4^\sigma - p_2^\rho p_4^\sigma - p_1^\rho p_3^\sigma + p_2^\rho p_3^\sigma - 2p_3^\rho p_4^\sigma)$
A_μ	$A_{H\nu}$	Φ^{++}	Φ^{--}	$\frac{4}{5} \frac{e^2}{c_w f^2} \varepsilon_{\mu\nu\rho\sigma} (p_1^\rho p_4^\sigma - p_2^\rho p_4^\sigma - p_1^\rho p_3^\sigma + p_2^\rho p_3^\sigma - 2p_3^\rho p_4^\sigma)$
A_μ	$W_{H\nu}^+$	Φ^+	Φ^{--}	$-2 \frac{e^2}{s_w f^2} \varepsilon_{\mu\nu\rho\sigma} (p_2^\rho p_4^\sigma - p_1^\rho p_3^\sigma + p_2^\rho p_3^\sigma - p_1^\rho p_4^\sigma)$
A_μ	$W_{H\nu}^+$	Φ^-	Φ^0	$\frac{e^2 \cdot \sqrt{2}}{s_w f^2} \varepsilon_{\mu\nu\rho\sigma} (3p_1^\rho p_3^\sigma + p_2^\rho p_4^\sigma - p_1^\rho p_4^\sigma - 3p_2^\rho p_3^\sigma + 4p_3^\rho p_4^\sigma)$
A_μ	$W_{H\nu}^+$	Φ^-	Φ^p	$\frac{ie^2 \cdot \sqrt{2}}{s_w f^2} \varepsilon_{\mu\nu\rho\sigma} (3p_1^\rho p_3^\sigma + p_2^\rho p_4^\sigma - p_1^\rho p_4^\sigma - 3p_2^\rho p_3^\sigma + 4p_3^\rho p_4^\sigma)$
A_μ	$W_{H\nu}^-$	Φ^+	Φ^0	$-\frac{e^2 \cdot \sqrt{2}}{s_w f^2} \varepsilon_{\mu\nu\rho\sigma} (p_2^\rho p_4^\sigma + 3p_1^\rho p_3^\sigma - 3p_2^\rho p_3^\sigma - p_1^\rho p_4^\sigma + 4p_3^\rho p_4^\sigma)$
A_μ	$W_{H\nu}^-$	Φ^+	Φ^p	$\frac{ie^2 \cdot \sqrt{2}}{s_w f^2} \varepsilon_{\mu\nu\rho\sigma} (p_2^\rho p_4^\sigma + 3p_1^\rho p_3^\sigma - 3p_2^\rho p_3^\sigma - p_1^\rho p_4^\sigma + 4p_3^\rho p_4^\sigma)$
A_μ	$W_{H\nu}^-$	Φ^{++}	Φ^-	$-2 \frac{e^2}{s_w f^2} \varepsilon_{\mu\nu\rho\sigma} (p_1^\rho p_4^\sigma - p_2^\rho p_3^\sigma + p_1^\rho p_3^\sigma - p_2^\rho p_4^\sigma)$
A_μ	$Z_{H\nu}$	Φ^+	Φ^-	$6 \frac{e^2}{s_w f^2} \varepsilon_{\mu\nu\rho\sigma} (p_1^\rho p_4^\sigma - p_2^\rho p_4^\sigma - p_1^\rho p_3^\sigma + p_2^\rho p_3^\sigma - 2p_3^\rho p_4^\sigma)$
A_μ	$Z_{H\nu}$	Φ^{++}	Φ^{--}	$4 \frac{e^2}{s_w f^2} \varepsilon_{\mu\nu\rho\sigma} (p_1^\rho p_4^\sigma - p_2^\rho p_4^\sigma - p_1^\rho p_3^\sigma + p_2^\rho p_3^\sigma - 2p_3^\rho p_4^\sigma)$
$A_{H\mu}$	W_ν^+	Φ^+	Φ^{--}	$\frac{2}{5} \frac{e^2}{c_w s_w f^2} \varepsilon_{\mu\nu\rho\sigma} (p_1^\rho p_4^\sigma - p_2^\rho p_4^\sigma + p_2^\rho p_3^\sigma - p_1^\rho p_3^\sigma + 2p_3^\rho p_4^\sigma)$
$A_{H\mu}$	W_ν^+	Φ^-	Φ^0	$\frac{1}{5} \frac{e^2 \cdot \sqrt{2}}{c_w s_w f^2} \varepsilon_{\mu\nu\rho\sigma} (p_1^\rho p_3^\sigma - p_2^\rho p_3^\sigma + p_2^\rho p_4^\sigma - p_1^\rho p_4^\sigma - 2p_3^\rho p_4^\sigma)$
$A_{H\mu}$	W_ν^+	Φ^-	Φ^p	$\frac{1}{5} \frac{ie^2 \cdot \sqrt{2}}{c_w s_w f^2} \varepsilon_{\mu\nu\rho\sigma} (p_1^\rho p_3^\sigma - p_2^\rho p_3^\sigma + p_2^\rho p_4^\sigma - p_1^\rho p_4^\sigma - 2p_3^\rho p_4^\sigma)$
$A_{H\mu}$	W_ν^-	Φ^+	Φ^0	$-\frac{1}{5} \frac{e^2 \cdot \sqrt{2}}{c_w s_w f^2} \varepsilon_{\mu\nu\rho\sigma} (p_2^\rho p_4^\sigma - p_1^\rho p_4^\sigma + p_1^\rho p_3^\sigma - p_2^\rho p_3^\sigma - 2p_3^\rho p_4^\sigma)$
$A_{H\mu}$	W_ν^-	Φ^+	Φ^p	$\frac{1}{5} \frac{ie^2 \cdot \sqrt{2}}{c_w s_w f^2} \varepsilon_{\mu\nu\rho\sigma} (p_2^\rho p_4^\sigma - p_1^\rho p_4^\sigma + p_1^\rho p_3^\sigma - p_2^\rho p_3^\sigma - 2p_3^\rho p_4^\sigma)$
$A_{H\mu}$	W_ν^-	Φ^{++}	Φ^-	$-\frac{2}{5} \frac{e^2}{c_w s_w f^2} \varepsilon_{\mu\nu\rho\sigma} (p_2^\rho p_4^\sigma - p_1^\rho p_4^\sigma + p_1^\rho p_3^\sigma - p_2^\rho p_3^\sigma - 2p_3^\rho p_4^\sigma)$
$A_{H\mu}$	Z_ν	Φ^+	Φ^-	$-\frac{2}{5} \frac{e^2 s_w}{c_w^2 f^2} \varepsilon_{\mu\nu\rho\sigma} (p_1^\rho p_4^\sigma - p_2^\rho p_4^\sigma - p_1^\rho p_3^\sigma + p_2^\rho p_3^\sigma + 2p_3^\rho p_4^\sigma)$
$A_{H\mu}$	Z_ν	Φ^{++}	Φ^{--}	$\frac{2}{5} \frac{(1-2s_w^2)e^2}{c_w^2 s_w f^2} \varepsilon_{\mu\nu\rho\sigma} (p_1^\rho p_4^\sigma - p_2^\rho p_4^\sigma - p_1^\rho p_3^\sigma + p_2^\rho p_3^\sigma + 2p_3^\rho p_4^\sigma)$
$A_{H\mu}$	Z_ν	Φ^0	Φ^p	$-\frac{2}{5} \frac{ie^2}{c_w^2 s_w f^2} \varepsilon_{\mu\nu\rho\sigma} (p_1^\rho p_3^\sigma - p_2^\rho p_3^\sigma - p_1^\rho p_4^\sigma + p_2^\rho p_4^\sigma - 2p_3^\rho p_4^\sigma)$
W_μ^+	$W_{H\nu}^+$	Φ^{--}	Φ^0	$-2 \frac{e^2 \cdot \sqrt{2}}{s_w^2 f^2} \varepsilon_{\mu\nu\rho\sigma} (p_1^\rho p_3^\sigma - p_2^\rho p_3^\sigma + p_2^\rho p_4^\sigma - p_1^\rho p_4^\sigma + 2p_3^\rho p_4^\sigma)$
W_μ^+	$W_{H\nu}^+$	Φ^{--}	Φ^p	$-2 \frac{ie^2 \cdot \sqrt{2}}{s_w^2 f^2} \varepsilon_{\mu\nu\rho\sigma} (p_1^\rho p_3^\sigma - p_2^\rho p_3^\sigma + p_2^\rho p_4^\sigma - p_1^\rho p_4^\sigma + 2p_3^\rho p_4^\sigma)$
W_μ^+	$W_{H\nu}^-$	h	h	$\frac{e^2}{s_w^2 f^2} \varepsilon_{\mu\nu\rho\sigma} (p_2^\rho p_3^\sigma - p_1^\rho p_3^\sigma + p_2^\rho p_4^\sigma - p_1^\rho p_4^\sigma)$
W_μ^+	$W_{H\nu}^-$	Φ^p	Φ^p	$-2 \frac{e^2}{s_w^2 f^2} \varepsilon_{\mu\nu\rho\sigma} (p_1^\rho p_3^\sigma - p_2^\rho p_3^\sigma + p_1^\rho p_4^\sigma - p_2^\rho p_4^\sigma)$

Table 11: T -parity violating vertices with two scalars and two gauge bosons. The momenta $p_{1,2,3,4}$ correspond to the particle in the first, second, third and fourth column, respectively. Continued in Tabs. 12 and 13

Particles				Vertices
W_μ^+	$Z_{H\nu}$	Φ^+	Φ^{--}	$4\frac{e^2}{s_w^2 f^2} \varepsilon_{\mu\nu\rho\sigma} p_4^\sigma (p_2^\rho - p_1^\rho + p_3^\rho)$
W_μ^+	$Z_{H\nu}$	Φ^-	Φ^0	$-2\frac{e^2 \cdot \sqrt{2}}{s_w^2 f^2} \varepsilon_{\mu\nu\rho\sigma} p_4^\sigma (p_1^\rho - p_2^\rho - p_3^\rho)$
W_μ^+	$Z_{H\nu}$	Φ^-	Φ^p	$-2\frac{ie^2 \cdot \sqrt{2}}{s_w^2 f^2} \varepsilon_{\mu\nu\rho\sigma} p_4^\sigma (p_1^\rho - p_2^\rho - p_3^\rho)$
W_μ^-	$W_{H\nu}^+$	h	h	$\frac{e^2}{s_w^2 f^2} \varepsilon_{\mu\nu\rho\sigma} (p_1^\rho p_3^\sigma - p_2^\rho p_3^\sigma + p_1^\rho p_4^\sigma - p_2^\rho p_4^\sigma)$
W_μ^-	$W_{H\nu}^+$	Φ^+	Φ^-	$2\frac{e^2}{s_w^2 f^2} \varepsilon_{\mu\nu\rho\sigma} (p_1^\rho p_4^\sigma - p_2^\rho p_4^\sigma + p_2^\rho p_3^\sigma - p_1^\rho p_3^\sigma - 2p_3^\rho p_4^\sigma)$
W_μ^-	$W_{H\nu}^+$	Φ^{++}	Φ^{--}	$-2\frac{e^2}{s_w^2 f^2} \varepsilon_{\mu\nu\rho\sigma} (p_2^\rho p_4^\sigma + 3p_1^\rho p_3^\sigma - 3p_2^\rho p_3^\sigma - p_1^\rho p_4^\sigma + 4p_3^\rho p_4^\sigma)$
W_μ^-	$W_{H\nu}^+$	Φ^0	Φ^0	$-2\frac{e^2}{s_w^2 f^2} \varepsilon_{\mu\nu\rho\sigma} (p_2^\rho p_3^\sigma - p_1^\rho p_3^\sigma + p_2^\rho p_4^\sigma - p_1^\rho p_4^\sigma)$
W_μ^-	$W_{H\nu}^+$	Φ^0	Φ^p	$4\frac{ie^2}{s_w^2 f^2} \varepsilon_{\mu\nu\rho\sigma} (p_1^\rho p_3^\sigma - p_1^\rho p_4^\sigma + p_2^\rho p_4^\sigma - p_2^\rho p_3^\sigma + 2p_3^\rho p_4^\sigma)$
W_μ^-	$W_{H\nu}^+$	Φ^p	Φ^p	$-2\frac{e^2}{s_w^2 f^2} \varepsilon_{\mu\nu\rho\sigma} (p_2^\rho p_3^\sigma - p_1^\rho p_3^\sigma + p_2^\rho p_4^\sigma - p_1^\rho p_4^\sigma)$
W_μ^-	$W_{H\nu}^-$	Φ^{++}	Φ^0	$-2\frac{e^2 \cdot \sqrt{2}}{s_w^2 f^2} \varepsilon_{\mu\nu\rho\sigma} (p_1^\rho p_4^\sigma - p_2^\rho p_4^\sigma + p_2^\rho p_3^\sigma - p_1^\rho p_3^\sigma - 2p_3^\rho p_4^\sigma)$
W_μ^-	$W_{H\nu}^-$	Φ^{++}	Φ^p	$2\frac{ie^2 \cdot \sqrt{2}}{s_w^2 f^2} \varepsilon_{\mu\nu\rho\sigma} (p_1^\rho p_4^\sigma - p_2^\rho p_4^\sigma + p_2^\rho p_3^\sigma - p_1^\rho p_3^\sigma - 2p_3^\rho p_4^\sigma)$
W_μ^-	$Z_{H\nu}$	Φ^+	Φ^0	$2\frac{e^2 \cdot \sqrt{2}}{s_w^2 f^2} \varepsilon_{\mu\nu\rho\sigma} p_4^\sigma (p_1^\rho - p_2^\rho - p_3^\rho)$
W_μ^-	$Z_{H\nu}$	Φ^+	Φ^p	$-2\frac{ie^2 \cdot \sqrt{2}}{s_w^2 f^2} \varepsilon_{\mu\nu\rho\sigma} p_4^\sigma (p_1^\rho - p_2^\rho - p_3^\rho)$
W_μ^-	$Z_{H\nu}$	Φ^{++}	Φ^-	$-4\frac{e^2}{s_w^2 f^2} \varepsilon_{\mu\nu\rho\sigma} (p_2^\rho p_3^\sigma - p_1^\rho p_3^\sigma - p_3^\rho p_4^\sigma)$
$W_{H\mu}^+$	Z_ν	Φ^+	Φ^{--}	$2\frac{e^2}{c_w s_w^2 f^2} \varepsilon_{\mu\nu\rho\sigma} (s_w^2 p_2^\rho p_4^\sigma - s_w^2 p_1^\rho p_4^\sigma + (2 - s_w^2) p_1^\rho p_3^\sigma - (2 - s_w^2) p_2^\rho p_3^\sigma - 2p_3^\rho p_4^\sigma)$
$W_{H\mu}^+$	Z_ν	Φ^-	Φ^0	$-\frac{e^2 \cdot \sqrt{2}}{c_w s_w^2 f^2} \varepsilon_{\mu\nu\rho\sigma} ((2 - 3s_w^2) p_2^\rho p_3^\sigma - (2 - 3s_w^2) p_1^\rho p_3^\sigma - s_w^2 p_1^\rho p_4^\sigma + s_w^2 p_2^\rho p_4^\sigma + 2(1 - 2s_w^2) p_3^\rho p_4^\sigma)$
$W_{H\mu}^+$	Z_ν	Φ^-	Φ^p	$-\frac{ie^2 \cdot \sqrt{2}}{c_w s_w^2 f^2} \varepsilon_{\mu\nu\rho\sigma} ((2 - 3s_w^2) p_2^\rho p_3^\sigma - (2 - 3s_w^2) p_1^\rho p_3^\sigma - s_w^2 p_1^\rho p_4^\sigma + s_w^2 p_2^\rho p_4^\sigma + 2(1 - 2s_w^2) p_3^\rho p_4^\sigma)$
$W_{H\mu}^-$	Z_ν	Φ^+	Φ^0	$-\frac{e^2 \cdot \sqrt{2}}{c_w s_w^2 f^2} \varepsilon_{\mu\nu\rho\sigma} (s_w^2 p_1^\rho p_4^\sigma - s_w^2 p_2^\rho p_4^\sigma - (2 - 3s_w^2) p_2^\rho p_3^\sigma + (2 - 3s_w^2) p_1^\rho p_3^\sigma - 2(1 - 2s_w^2) p_3^\rho p_4^\sigma)$
$W_{H\mu}^-$	Z_ν	Φ^+	Φ^p	$\frac{ie^2 \cdot \sqrt{2}}{c_w s_w^2 f^2} \varepsilon_{\mu\nu\rho\sigma} (s_w^2 p_1^\rho p_4^\sigma - s_w^2 p_2^\rho p_4^\sigma - (2 - 3s_w^2) p_2^\rho p_3^\sigma + (2 - 3s_w^2) p_1^\rho p_3^\sigma - 2(1 - 2s_w^2) p_3^\rho p_4^\sigma)$
Z_μ	$Z_{H\nu}$	Φ^0	Φ^p	$2\frac{ie^2}{c_w s_w^2 f^2} \varepsilon_{\mu\nu\rho\sigma} (p_1^\rho p_3^\sigma - p_2^\rho p_3^\sigma - p_1^\rho p_4^\sigma + p_2^\rho p_4^\sigma + 2p_3^\rho p_4^\sigma)$

Table 12: (Continuation of Tab. 11) T -parity violating vertices with two scalars and two gauge bosons. The momenta $p_{1,2,3,4}$ correspond to the particle in the first, second, third and fourth column, respectively. Continued in Tab. 13

Particles				Vertices
$W_{H\mu}^-$	Z_ν	Φ^{++}	Φ^-	$-2\frac{e^2}{c_w s_w^2 f^2} \varepsilon_{\mu\nu\rho\sigma} ((2 - s_w^2) p_1^\rho p_4^\sigma - (2 - s_w^2) p_2^\rho p_4^\sigma + s_w^2 p_2^\rho p_3^\sigma - s_w^2 p_1^\rho p_3^\sigma + 2 p_3^\rho p_4^\sigma)$
Z_μ	$Z_{H\nu}$	Φ^+	Φ^-	$6\frac{c_w e^2}{s_w^2 f^2} \varepsilon_{\mu\nu\rho\sigma} (p_1^\rho p_4^\sigma - p_2^\rho p_4^\sigma - p_1^\rho p_3^\sigma + p_2^\rho p_3^\sigma - 2 p_3^\rho p_4^\sigma)$
Z_μ	$Z_{H\nu}$	Φ^{++}	Φ^{--}	$2\frac{(1-2s_w^2)e^2}{c_w s_w^2 f^2} \varepsilon_{\mu\nu\rho\sigma} (p_1^\rho p_4^\sigma - p_2^\rho p_4^\sigma - p_1^\rho p_3^\sigma + p_2^\rho p_3^\sigma - 2 p_3^\rho p_4^\sigma)$
W_μ^+	$W_{H\nu}^-$	Φ^+	Φ^-	$-2\frac{e^2}{s_w^2 f^2} \varepsilon_{\mu\nu\rho\sigma} (p_2^\rho p_4^\sigma - p_1^\rho p_4^\sigma + p_1^\rho p_3^\sigma - p_2^\rho p_3^\sigma + 2 p_3^\rho p_4^\sigma)$
W_μ^+	$W_{H\nu}^-$	Φ^{++}	Φ^{--}	$2\frac{e^2}{s_w^2 f^2} \varepsilon_{\mu\nu\rho\sigma} (3 p_1^\rho p_4^\sigma + p_2^\rho p_3^\sigma - p_1^\rho p_3^\sigma - 3 p_2^\rho p_4^\sigma - 4 p_3^\rho p_4^\sigma)$
W_μ^+	$W_{H\nu}^-$	Φ^0	Φ^0	$-2\frac{e^2}{s_w^2 f^2} \varepsilon_{\mu\nu\rho\sigma} (p_1^\rho p_3^\sigma - p_2^\rho p_3^\sigma + p_1^\rho p_4^\sigma - p_2^\rho p_4^\sigma)$
W_μ^+	$W_{H\nu}^-$	Φ^0	Φ^p	$-4\frac{ie^2}{s_w^2 f^2} \varepsilon_{\mu\nu\rho\sigma} (p_2^\rho p_3^\sigma - p_2^\rho p_4^\sigma + p_1^\rho p_4^\sigma - p_1^\rho p_3^\sigma - 2 p_3^\rho p_4^\sigma)$

Table 13: (Continuation of Tab. 12) T -parity violating vertices vertices two scalars and two gauge bosons. The momenta $p_{1,2,3,4}$ correspond to the particle in the first, second, third and fourth column, respectively.

References

- [1] N. Arkani-Hamed, A. G. Cohen, E. Katz and A. E. Nelson, JHEP **0207**, 034 (2002).
- [2] C. Csaki, J. Hubisz, G. D. Kribs, P. Meade and J. Terning, Phys. Rev. D **67**, 115002 (2003);
J. L. Hewett, F. J. Petriello and T. G. Rizzo, JHEP **0310**, 062 (2003);
C. Csaki, J. Hubisz, G. D. Kribs, P. Meade and J. Terning, Phys. Rev. D **68**, 035009 (2003);
W. Kilian and J. Reuter, Phys. Rev. D **70**, 015004 (2004).
- [3] J. Wudka, hep-ph/0307339.
- [4] H. C. Cheng and I. Low, JHEP **0408**, 061 (2004).
- [5] C. T. Hill and R. J. Hill, Phys. Rev. D **75**, 115009 (2007).
- [6] C. T. Hill and R. J. Hill, Phys. Rev. D **76**, 115014 (2007).
- [7] J. Wess and B. Zumino, Phys. Lett. B **37**, 95 (1971);
E. Witten, Nucl. Phys. B **223**, 422 (1983).
- [8] D. Krohn and I. Yavin, arXiv:0803.4202 [hep-ph].
- [9] C. Csaki, J. Heinonen, M. Perelstein and C. Spethmann, arXiv:0804.0622 [hep-ph].
- [10] V. Barger, W. Y. Keung and Y. Gao, Phys. Lett. B **655**, 228 (2007).

- [11] J. Hubisz and P. Meade, Phys. Rev. D **71**, 035016 (2005).
- [12] M. Blanke, A. J. Buras, A. Poschenrieder, S. Recksiegel, C. Tarantino, S. Uhlig and A. Weiler, JHEP **0701**, 066 (2007).
- [13] I. Low, JHEP **0410**, 067 (2004).
- [14] E. Katz, J. y. Lee, A. E. Nelson and D. G. E. Walker, JHEP **0510** (2005) 088.
- [15] A. Pukhov, arXiv:hep-ph/0412191.
- [16] A CALCHEP model file for the Littlest Higgs model with broken T-parity
<http://www.itp.uzh.ch/~pedro/lht/>.
- [17] A. Denner, G. Weiglein and S. Dittmaier, Phys. Lett. B **333** (1994) 420.
- [18] R. S. Hundi, B. Mukhopadhyaya and A. Nyffeler, Phys. Lett. B **649**, 280 (2007)
- [19] M. S. Carena, J. Hubisz, M. Perelstein and P. Verdier, Phys. Rev. D **75** (2007) 091701.
- [20] Vista/Sleuth Global Search for New Physics in 2.0 fb-1 of p-pbar Collisions at $\sqrt{s}=1.96$ TeV,
http://www-cdf.fnal.gov/physics/exotic/r2a/20080228.vista_sleuth/publicPage.html
- [21] A. Freitas and D. Wyler, JHEP **0611** (2006) 061
- [22] A. Belyaev, C. R. Chen, K. Tobe and C. P. Yuan, Phys. Rev. D **74** (2006) 115020
- [23] J. Hubisz, S. J. Lee and G. Paz, JHEP **0606**, 041 (2006).
- [24] C. R. Chen, K. Tobe and C. P. Yuan, Phys. Lett. B **640** (2006) 263
- [25] J. Gasser and H. Leutwyler, Nucl. Phys. B **250**, 517 (1985).
- [26] J. F. Donoghue and D. Wyler, Nucl. Phys. B **316**, 289 (1989).
- [27] M. J. Savage, M. E. Luke and M. B. Wise, Phys. Lett. B **291** (1992) 481
- [28] T. Han, H. E. Logan, B. McElrath and L. T. Wang, Phys. Rev. D **67**, 095004 (2003).
- [29] W. Y. Keung, I. Low and J. Shu, arXiv:0806.2864 [hep-ph].
- [30] A. Denner, Fortsch. Phys. **41** (1993) 307